

AD \_\_\_\_\_

Award Number: DAMD17-98-1-8309

TITLE: Development and Clinical Evaluation of Tomosynthesis for  
Digital Mammography

PRINCIPAL INVESTIGATOR: Daniel B. Kopans, M.D.

CONTRACTING ORGANIZATION: The General Hospital Corporation  
Boston, Massachusetts 02114

REPORT DATE: October 2000

TYPE OF REPORT: Annual

PREPARED FOR: U.S. Army Medical Research and Materiel Command  
Fort Detrick, Maryland 21702-5012

DISTRIBUTION STATEMENT: Approved for public release;  
Distribution unlimited

The views, opinions and/or findings contained in this report are those of the author(s) and should not be construed as an official Department of the Army position, policy or decision unless so designated by other documentation.

20010323 108

**REPORT DOCUMENTATION PAGE**

OMB No. 074-0188

Public reporting burden for this collection of information is estimated to average 1 hour per response, including the time for reviewing instructions, searching existing data sources, gathering and maintaining the data needed, and completing and reviewing this collection of information. Send comments regarding this burden estimate or any other aspect of this collection of information, including suggestions for reducing this burden to Washington Headquarters Services, Directorate for Information Operations and Reports, 1215 Jefferson Davis Highway, Suite 1204, Arlington, VA 22202-4302, and to the Office of Management and Budget, Paperwork Reduction Project (0704-0188), Washington, DC 20503

<b>1. AGENCY USE ONLY (Leave blank)</b>		<b>2. REPORT DATE</b> October 2000	<b>3. REPORT TYPE AND DATES COVERED</b> Annual (30 Sep 99 - 29 Sep 00)	
<b>4. TITLE AND SUBTITLE</b> Development and Clinical Evaluation of Tomosynthesis for Digital Mammography			<b>5. FUNDING NUMBERS</b> DAMD17-98-1-8309	
<b>6. AUTHOR(S)</b> Daniel B. Kopans, M.D.				
<b>7. PERFORMING ORGANIZATION NAME(S) AND ADDRESS(ES)</b> The General Hospital Corporation Boston, Massachusetts 02114  <b>E-MAIL:</b> kopans.daniel@mgh.harvard.edu			<b>8. PERFORMING ORGANIZATION REPORT NUMBER</b>	
<b>9. SPONSORING / MONITORING AGENCY NAME(S) AND ADDRESS(ES)</b> U.S. Army Medical Research and Materiel Command Fort Detrick, Maryland 21702-5012			<b>10. SPONSORING / MONITORING AGENCY REPORT NUMBER</b>	
<b>11. SUPPLEMENTARY NOTES</b>				
<b>12a. DISTRIBUTION / AVAILABILITY STATEMENT</b> Approved for public release; Distribution unlimited				<b>12b. DISTRIBUTION CODE</b>
<b>13. ABSTRACT (Maximum 200 Words)</b>  Tomosynthesis holds the promise of detecting breast cancer earlier, at a smaller size, with fewer false-positive outcomes. Progress toward this goal has been steady. It has been slowed by the unanticipated need to include an articulating collimator for X-ray beam control. GECDR interpreted recent FDA guidance as requiring the design and installation of an articulating collimator. GECDR has designed and installed this subsystem. The feasibility automatic motorized tomosynthesis system has been delivered, installed and acceptance tested at MGH. A physics report on the imaging characteristics is complete. We are now in position to evaluate tomosynthesis in the clinical setting. This will permit an understanding of it's clinical potential, and if warranted, the design of a clinical trial.  Conclusion  We have constructed a workable system and have begun to establish clinical feasibility by conducting a preliminary clinical evaluation.				
<b>14. SUBJECT TERMS</b> Breast Cancer, Tomosynthesis, 3D Imaging, Cancer detection			<b>15. NUMBER OF PAGES</b> 91	
			<b>16. PRICE CODE</b>	
<b>17. SECURITY CLASSIFICATION OF REPORT</b> Unclassified	<b>18. SECURITY CLASSIFICATION OF THIS PAGE</b> Unclassified	<b>19. SECURITY CLASSIFICATION OF ABSTRACT</b> Unclassified	<b>20. LIMITATION OF ABSTRACT</b> Unlimited	

NSN 7540-01-280-5500

Standard Form 298 (Rev. 2-89)  
Prescribed by ANSI Std. Z39-18  
298-102

<b>Table of Contents</b>	<b>page</b>
<b>1 Front Cover Page</b>	<b>1</b>
<b>2 Report Documentation Page (SF 298)</b>	<b>2</b>
<b>3 Table of Contents</b>	<b>3</b>
<b>4 Introduction</b>	<b>4</b>
<b>5 Body</b>	<b>5</b>
<b>6 Key Research Accomplishments</b>	<b>21</b>
<b>7. Reportable Outcomes</b>	<b>21</b>
<b>8. Conclusions</b>	<b>22</b>
<b>9 Reference</b>	<b>23</b>
<b>10. Figures</b>	<b>24</b>
<b>11 Appendices</b>	<b>35</b>
<b>Appendix 1: Report “Out of plane Structure Removal”</b>	<b>35</b>
<b>Appendix 2: Physicist Evaluation –Acceptance test</b>	<b>49</b>
<b>Appendix 3: FFDM Tomosynthesis User’s Manual</b>	<b>68</b>
<b>Appendix 4: Patent Application by GECRD</b>	<b>85</b>

## **4 Introduction**

Tomosynthesis holds the promise of detecting breast cancer earlier, at a smaller size, with fewer false-positive outcomes. The purpose of this development effort is to advance Tomosynthesis by constructing a workable system and establishing clinical feasibility by conducting a preliminary clinical evaluation.

This annual report will (1) summarize the current state of Tomosynthesis development, (2) review issues that surfaced during the second year of development and (3) summarize the plans for the upcoming year.

## **5 Body: Progress of the Tomosynthesis Development Project**

General Electric (GE) and the Breast Imaging Division of Massachusetts General Hospital (BIMGH) have conducted a development effort which has resulted in a clinical feasibility prototype Tomosynthesis system. It is hoped that this system will permit a meaningful assessment of the advantages of tomosynthesis in the clinical setting.

The clinical feasibility prototype Tomosynthesis system has been constructed at General Electric Corporate Research and Development facilities in Niskayuna, NY during the first two years of this three-year project plan. It is comprised of an extensively modified General Electric (GE) DMR clinical mammography system, equipped with integrated automatic motion and exposure control subsystems.

Trips were made between Boston, MA, Niskayuna, NY, and Hillsborough, NC by Dr. Niklason, Dr. Opsal-Ong, Dr. Eberhard and Mr. Moore to perform Tomosynthesis experiments, and make measurements to refine the mechanical design, clinical experimental design and overall goals of the project.

### *Design*

#### Articulating collimator

An unplanned design cycle was initiated to comply with GE's interpretation of FDA radiation protection criteria which resulted in implementing an articulated beam-collimator that actively synchronizes with tube-head position to illuminate just the detector area with X-rays at all positions.

### *Experiments*

#### Vibration testing

GE quantified the success of the stand-vibration reduction program with extensive accelerometry, showing that image quality should not be adversely affected.

As reported in the previous progress report, MTF system analysis demonstrates a retention of the inherent MTF in-plane and -focus plane is less than 2 mm.

In addition to the mechanical aspects of design, we have been working to determine the optimal reconstruction algorithm. We have been able to proceed in parallel with development based on manually acquired mastectomy datasets reconstructed to evaluate image characteristics. The analysis of this series of 25 mastectomy datasets, collected under a previous ARMY-funded (ARMY BC970208), employing manual positioning is used to guide the initial clinical acquisition protocols

GE has interpreted FDA guidance as requiring GE to design and install a motorized-automatic collimator to control beam radiation on the prototype system. This has delayed the delivery date by some about 7 months.

GE CRD submitted this report electronically, dated 13-Oct-2000 to MGH to meet their contractual obligation:

## **FFDM Tomosynthesis System 2000 CRD Annual Report**

### **1. Introduction**

The tomosynthesis prototype system was installed at Massachusetts General Hospital on August 9 and 10, 2000. The complete system (except for the Image Review Workstation) was shipped by air suspension moving van from Schenectady, NY, to Boston. The Full Field Digital Mammography system at MGH was de-installed and returned to GE CRD. The system was successfully brought up, and initial digital tomosynthesis images were acquired with the system at MGH on August 10, 2000.

More comprehensive system validation testing was carried out at MGH on September 5 - 7, 2000. Testing consisted of acquiring tomosynthesis images of phantoms at all the x-ray techniques available on the system for tomosynthesis. Scans were acquired in approximately 35 different imaging configurations, with a reliability rate in excess of 97%. Detailed characterization of the system functional characteristics (dose, linearity, half value layer, collimation, etc.) were also successfully carried out (See Appendix 2. In summary, "the tomosynthesis unit is performing well and is ready for initial patient imaging"[1].

### **2. System Development and Integration**

#### **2.a. Out of Plane De-Blurring Algorithms**

The "standard" tomosynthesis reconstruction algorithm is the shift-and-add algorithm, which is the digital equivalent of the image formation process in conventional tomography imaging. In terms of reconstruction artifacts, we see some significant differences between digital tomosynthesis and conventional tomography. In particular, the characteristics of the out-of-plane structures appear in the reconstruction is dramatically different. In conventional tomography both detector and tube undergo a coordinated continuous movement during the exposure, such that only the fulcrum plane (i.e., the plane of interest) is projected onto the exact same location of the film, while projections of other planes change their relative position with respect to the film. Obviously this leads to a "continuous" blurring of the out-of-plane structures, which decreases the perceived contrast of these structures relative to the structures located in the

fulcrum plane. Furthermore, the larger the distance of a structure from the fulcrum plane, the more blurred it is, which in turn reduces the contrast of the artifacts produced. In digital tomosynthesis, however, the situation is different. Here we only have a limited number  $N$  of images, typically  $N=8$  or  $11$  in our tomosynthesis prototype for breast imaging. The shift and add reconstruction algorithm consists of shifting and scaling the projection images such that structures in the target slice line up in all projections, and then averaging over all images (see Figure 2.1). An out-of-plane structure will appear in every single projection image, and the reconstructed slice will therefore contain  $N$  low-contrast images of this structure. Depending on the size of the structure and the angular distribution of the tube positions for image acquisition, these copies will overlap in reconstructed slices which are close to the true location of this structure, but with increasing distance of the reconstructed slice from the true object location they will appear as separate copies, with low contrast. Note here that we reach the point where an out-of-plane structure appears in form of a number of separate, non-overlapping copies, every reconstructed slice which has an even larger distance from the considered structure will again contain  $N$  copies of the structure, with a constant contrast. That is, unlike in conventional tomography, the contrast of out-of-plane structures decreases as a function of the distance from the fulcrum plane only up to a certain distance, after which the contrast remains constant. Furthermore, this “limit-contrast”, i.e., the lowest contrast an out-of-plane structure can have, is  $1/N$  of the contrast of that same structure when “in focus”. Dictated by the low number of images we are using in our system, this contrast is at about 10 percent of the contrast of the original structure. For high contrast calcifications, this may create artifacts which are clearly visible in all reconstructed slices. These facts motivate the search for an algorithmic approach to remove out-of-plane structures in digital tomosynthesis.

We have evaluated a number of approaches found in the literature to remove this type of artifact, where we focused on the specific system characteristics encountered in the prototype tomosynthesis system for breast imaging. These approaches can be roughly classified into four classes:

#### **2.a.i. Direct inverse filtering [2,3]**

The projection mapping, and the subsequent “backprojection” performed in the shift and add reconstruction suggest a “star-shaped” point spread function. If we have a single point-like structure in the considered volume, then this point will be visible on each projection image, and the shift and add reconstruction will generate  $N$  copies of this point in each reconstructed slice. These copies line up at the object height, and they are further and further apart the farther away from the object height we examine. What was a single point in the original volume now has a star shaped structure in the  $z$ -direction of the reconstruction (see Figure 2.2). One can therefore assume that the shift and add reconstruction results in the structure of the original 3D volume, but now convolved (or filtered) with the star-shaped point spread function.

Filtering translates into a product of the spectra in the Fourier domain. The inverse filtering approach consists of computing the Fourier transform of the shift and

add reconstructed volume, dividing by the spectrum of the (known) point spread function, and then performing the inverse Fourier transform. In practice this approach presents several problems. First, the spectrum of the point spread function has some regions where it is zero, and it has also a number of small values. At these points it is either impossible to compute this division, or the result will potentially be very noisy. Therefore, this “reconstruction” cannot recover the full structure of the object. Second, the assumption that we have a uniquely defined point spread function is only true for a parallel beam projection, but not for a cone beam projection as in our system. Due to these limitations, as well as discretization issues, one observes that the performance of this algorithm in terms of image quality improvement, is not satisfactory. It should be noted, however, that although this approach requires and uses the whole reconstructed volume, this algorithm is tractable even for relatively large datasets, mainly due to the efficiency of the FFT.

### **2.a.ii. Image post-processing / Unsharp-masking [4,5]**

The underlying assumption of this approach is the fact that out-of-plane structures appear as somewhat “blurred” copies of themselves. Furthermore, one assumes that additional blurring of a reconstructed slice will leave out-of-plane structures essentially unchanged. That means that we can now subtract the blurred version from the originally reconstructed slice, thereby removing the out-of-plane structures. “Blurring-and-subtracting” is essentially a high-pass filtering, therefore this procedure enhances high frequency structures in the reconstructed slice. As we discussed earlier, the observed “blurring” of out-of-plane structures is not continuous in our digital tomosynthesis framework. In addition, the “spread” of the distinct copies of out-of-plane structures depends on the distance of these structures from the reconstructed plane. Both of these effects illustrate why this approach may be useful in somewhat enhancing the perceived image quality, and, for a given slice, it may be possible to design a filter which suppresses most of the out-of-plane structures. However, this approach (with a fixed filter) cannot be effective in removing out-of-plane structures overall. In particular, it will act in a similar fashion on “separate” (i.e., non-overlapping) copies of out-of-plane structures, as it does on in-plane structures. Either both are enhanced, or both are suppressed. The resulting images show in general an enhanced contrast (due to the high-pass filter characteristic), while the out-of-plane structures (depending on their frequency characteristic) may also be enhanced. However, for specific cases, or single slices, this method may be of some value, in particular through the fact that it is easy to implement, and acts on a single slice, i.e., it does not require a large amount of memory.

### **2.a.iii. Iterative updates of reconstructed volume [6,7,8]**

The approach here is to use an iterative update of the reconstructed volume, which converges to a solution of the “projection equation”. Specifically, one assumes that the shift-and-add reconstruction is a “reasonable” estimate of the true underlying three-dimensional object. In that sense, computing the projection of the difference between true object and current estimate, and then performing a shift and add reconstruction of this “projected error”, gives a reasonable estimate of the error – which can then be used to

update the current estimate. In practice, the true object is of course not available, but only its projections. Because both projection and shift-and-add reconstruction are linear, it is sufficient to compute projection and reconstruction of the current estimate of the object, then compute the difference to the reconstruction from the original projection data, and update the current estimate with that difference. This approach is equivalent to the strategy given in the motivation above. This method is one of the more promising approaches in our comparative study. It is a method which converges theoretically, and which does not suffer from modeling errors as, for example, the direct inverse filtering approach does. Simulations have shown that this method performs relatively well when compared to the other approaches. However, it does not fully remove the out-of-plane artifacts, and due to the fact that it explicitly uses the full reconstructed volume, the amount of memory as well as the computational power required are extremely high, and prohibit the use of this method for real data sets.

#### **2.a.iv. One-step updates using information from neighboring slices [9]**

The motivation for this approach lies in the fact that, if some slice through the object is known exactly, then the contribution of this slice to the out-of-plane artifacts in the (shift-and-add) reconstruction of any other slice can be determined exactly, and then removed (subtracted) from the reconstruction. An approximation of this approach uses neighboring slices as reconstructed using the shift-and-add algorithm, and subtracts their "contribution" to out-of-plane structures in the target slice. This approach cannot be used in an iterative fashion, because it does not converge. Obviously, in order to have an optimal removal of out-of-plane artifacts, this approach requires using all slices. This is of particular importance, because, as we discussed earlier, the contrast of out-of-plane structures does not decrease as a function of the distance. This requirement makes the computational effort and amount of memory excessive for use on real data sets. The performance of this approach in simulations seems to be slightly superior to the direct inverse filtering and unsharp-masking approaches, although it creates some undesirable artifacts in form of significant low-frequency variations in the reconstructed volume.

#### **2.a.v. Filtered Backprojection**

Although not formally included in our comparison of techniques to remove out-of-plane structures, filtered back projection can be viewed as a tool for doing just this. The motivation for using filtered backprojection in tomosynthesis is derived from its wide application in CT. There the filtering step does indeed correct for artifacts, as it compensates for the circularly symmetric point-spread function with a  $1/r$  characteristic, which would result from a simple backprojection reconstruction approach. Unfortunately, this argument does not hold in our framework, as we have only a small number of projections, with a small angular range. The effects and drawbacks of filtered backprojection in our case are somewhat similar to the unsharp-masking approach. The main effect is an enhancement of the high-frequency content of the images (which may lead to a perceived improvement in image quality for images or image regions with certain characteristics), and it may cancel some of the out-of-plane artifacts for some of

the reconstructed slices. However, it can be observed that high-frequency out-of-plane structures are also enhanced, which means that filtered backprojection cannot qualify as an effective tool for removal of out-of-plane artifacts.

#### **2.a.vi. Summary of results**

In summary one can say that no one of the investigated methods shows a satisfactory performance in removing out-of-plane structures. Some methods have only very limited success in removing out-of-plane artifacts, and are also sensitive to noise (direct inverse filtering, unsharp-masking, filtered backprojection), but they are fast and efficient to implement. Other methods show only a slightly better performance in terms of image quality, but this comes at the expense at the additional expense of immense computational cost (iterative as well as one-step updates), and also the introduction of additional artifacts (one-step updates). For more details see the results presented in the Appendix 1.

#### **2.b. Tomo Prototype Software**

The prototype software for the Tomosynthesis prototype is an application that runs on the UNIX platform, and uses the X Window system for user interaction. The software is a modification of the prototype software for the Full Field Digital Mammography (FFDM) prototype. The baseline software, the Digital Mammography System (DMS) version 2.8, was modified to add the functionality required for the tomosynthesis prototype. The software consists of two primary parts: the user interface portion and the system software. The user interface portion allows the user to interact with the prototype device and software using a Graphical User Interface (GUI). The system software, in turn, communicates and controls the various devices in the system to operate the scanner, etc.

##### **Modifications to the DMS GUI**

The DMS GUI has been modified in three ways:

- Addition of new GUI features to support tomo-acquisition: examples include a new tomo technique editor, scan plan selection, custom tomo scan creation, etc.
- Removal of redundant or unsupported features from the FFDM prototype: examples include removal of non-functional and unsupported functions from the QC (Quality Check) menu.
- Replacement of some GUI features with updated versions: examples include a new archive system that automates the entire archive procedure.

##### **Modifications to the DMS systems software**

The DMS system software has been extensively modified to operate the tomosynthesis prototype. Modifications include:

- Addition of reconstruction processing.
- Modification of image transfer and manipulation software to handle tomo images.
- Addition of new acquisition codes for the tomo acquisition modes.

### **2.c. Asymmetric Collimator**

Modification of a DMR system for tomosynthesis requires a new asymmetric collimator to satisfy CDRH 21CRF1020.31(m). On the DMR, the pivot point for x-ray tube rotation is approximately 20 cm above the detector. When the tube arm is not perpendicular to the detector, using the standard collimator causes the x-ray beam to not completely fill the detector on the side it is tilted toward, while spilling off on the other side. To overcome this deficiency, the standard collimator was replaced by an asymmetric collimator which could be shifted from side to side via a servomotor controlled by the motion controller used to move the tube. An analysis was performed to show that this was feasible from an x-ray field of view standpoint [10], and servo components were selected that could move the 20 mil tungsten plate from position to position in the required time. The servo controller had been selected to have enough axes to control a fixed aperture collimator in addition to the x-ray tube motion. It can control these axes on separate threads, so the tube and collimator can be moved at the same time. Tests were performed using the motion controller's position capture capability to show that both the collimator motion as well as the tube motion were complete in the required time.

An alignment jig was manufactured from a graphite plate by machining it so it fit precisely into the opening in the collimator. Several sets of tungsten wires were glued into slots cut into the graphite for use in determining the position of the collimator cut-off even if it fell off the detector. The position of these wires relative to the collimator opening were determined by taking a digital x-ray of the jig while it was placed in the compression paddle in a raised position, allowing magnification of the jig. Relationships were then mathematically obtained to allow computation of the collimator edges from the wire positions in the field of view. After the detector had been aligned so that the rotation axis of the tube was parallel to the row direction of the imager, the chest wall cut-off was adjusted using the wires parallel to the chest wall edge. Then for each angle of use, a digital image was obtained and the collimator position adjusted until the x-ray cutoff was within the specified percentage of SID.

Safety features of the collimator operation include checking the collimator and tube positions at the end of a move against the expected positions, so that if they are off more than a small error tolerance, the x-ray exposure is aborted. This will prevent radiation spill if the collimator position is not matched to the tube position, allowing radiation to fall off one side or other. Tests were performed to verify the operation of this feature.

### **2.d. Mechanical Techniques to Minimize Vibration**

#### 2.d.i. Base Plate

One of the main sources of vibration was the original base that supported the DMR elevating column. The base was only ½" thick and while this is more than enough for the static load of the DMR it was not sufficient when the tube was under motion. We resolved the problem by making a larger and thicker sub-base. The sub-base was plug welded to the original base, in strategic locations from underneath to stabilize the base and minimize column deflection and vibration.

#### 2.d.ii. Aluminum Bars inside the DMR Column

The second source of vibration was found within the column itself. The interior of the column contains two linear bearings, a ball-screw, and two roller bearing guides. The roller bearing guides were inadequate for our application. We remedied the problem by bolting two aluminum bars inside the column as a fixed spacer. This solution, unfortunately, eliminated the variable height adjustment of the DMR column. We placed holes in given increments on the outer wall of the column to allow for height adjustment.

#### 2.d.iii. Modified Ball Screw

Our first approach for the ball-screw drive that drives the movement of the tube suffered from too many free moving mechanical connections, or degrees of freedom. There was a certain amount of torque and moment, associated with the drive configuration in the first attempt, which created an oscillation at each start and stop of the drive. We eliminated an entire kinetic link, improving the drive system considerably. The drive will now allow for image quality that is well within the specs required.

#### 2.d.iv. X-Ray Tube Cowling

The cowling, or bonnet, required in shielding the patient from moving parts and x-rays was ultimately redesigned and fabricated of polyurethane foam fiberglass laminate. This material served to be lightweight but yet durable enough for the clinical setting. The interior was also lined with a layer of thin lead to protect the patient from unwanted x-ray exposure. The construction of this part also allows for easy field service access in the event that components need repair.

### 2.e. Techniques for Tomosynthesis

#### 2.e.i. Timing Model

System timing is critical in the performance of the tomosynthesis prototype, since the x-ray dose must be divided into 8 or 11 very short exposures, compatible with both the mAs values available on the DMR and the requirements of the detector read-out timing. Therefore, a new timing model was developed for the tomosynthesis prototype. The new model allows for accurate prediction and control of X-ray expose time in each

frame. The timing model accounts for interactions between the data acquisition computer, the DMR system and the motion controller. All three of these systems interact to control the on-time for the X-ray tube. Using the timing model allows for new timing modes, corresponding to novel techniques, to be rapidly developed and tested. Experimental data, based on repeated runs of the system in a testing configuration, were used to validate the timing model.

#### 2.e.ii. Technique choices, scan plans, views etc.

For evaluation of the utility of tomosynthesis in x-ray mammography examinations, the system was constructed to allow evaluation of different angular ranges (40 and 50 degrees), different number of angles (8 or 11) of exposure, and different target/filter combinations (Mo/Mo, Mo/Rh, Rh/Rh). A smaller angular range reduces the tube move distance and hence system vibration for a given number of angles, while a larger range gathers more information (allows greater discrimination between objects in the focal plane and those not). The larger range also has a corresponding smaller depth of field, so that spacing of the reconstruction planes must be smaller. Mo/Mo has been favored for thin breasts for reasons of better image contrast, but if reduced compression is an objective, or for a larger angular range (which passes radiation through the breast at higher angles to normal), the more penetrating Mo/Rh and Rh/Rh techniques are favored. The specific choices available on the tomosynthesis prototype are listed in Chapter 2 of Appendix 3.

#### 2.f. IQ Tools to Characterize Performance

The major concern in terms of image quality was the residual vibration of the system after movement of the x-ray tube. This is a potentially important factor, since in tomosynthesis mode every single projection image (with the exception of the first image) is acquired immediately after the tube is being moved. The requirement to keep an exam as short as possible to reduce compression time for the patient, limits the elapsed time between tube movement and acquisition of the next image. For these reasons, the amount of vibration during the exposure, and in particular its impact on image quality, has to be carefully evaluated.

The impact of vibration on image quality was quantified by imaging steel spheres (ball bearings, or BB's) with a diameter of approximately 2 mm. In an image acquired without any system vibration (or any other sources of blur), the "shadow" of the BB will be shaped like an ellipse, with very sharp and well-defined edges. The grayscale profile across the edge will be a step function. The stronger the blur in the image, the more blurred the edge of the BB will be, and the grayscale profile across the edge of the blurred BB will be a more gradual function, not a step function. Evaluating the blur of the image involves finding the shadow of the BB, identifying its edges and extracting grayscale profiles across the edge, and quantifying the difference between the profile and an ideal step function.

In particular, the amount of blur was quantified by finding an “optimal fit” of the considered edge profile with a step function, normalizing both functions, and computing the area between the two curves, as illustrated in Figure 2.3. The resulting value, which represents our measure of blur, can be interpreted as being the standard deviation of a Gaussian blurring kernel, or the half of the full-width-half-max (FWHM) value of a blurring kernel (in number of pixels). Obviously, in cases where we have almost no blurring, i.e., when the edge is “spread out” over only very few pixels, the “blurring measure” can vary due to quantization effects due to the pixel grid of the detector (that is, for values smaller than 1), while the determined blur value is significantly more reliable for values larger than 1.

The measurements of vibration/blur were carried out separately both in the scan direction, and orthogonal to it, in order to evaluate blur/vibration in all directions. In Figure 2.4 we illustrate the connection between images and the associated measures of blur by showing images of BB's, the associated grayscale profiles across the edges, and the corresponding results for the measure of blur.

Note that, in order to have a good image quality in the tomosynthesis reconstruction, it is by no means required to have optimal image quality for every single projection image. In fact, if only two or three out of 10 or 11 images have a noticeable blur, then the image quality of the reconstruction will be far superior to the image quality of the single “blurred” projection images.

## **2.g. Final Tomo System Configuration**

In evaluating the system for effects on image quality due to vibration, it became clear that the vibration was worse at the highest rate (minimum move time), and better with slower, smoother moves. The minimum rate is set by the detector read-out time (300 milliseconds), and the maximum rate by the register size of the DMR for tube spit time-out (655 ms). The moment of inertia of the tube arm and servo-drive are such that while the servomotor is capable of performing the move, the amplifier used is not, and the move is not smooth and hence has frequency components that excite system vibrations [10]. A move time of 600 milliseconds was determined to be optimal. With 11 angles (10 moves) and a dose requiring two seconds to deliver, this results in a total exam time of 8 seconds. This does not include positioning time by the technologist.

Tests were run imaging 2 millimeter diameter steel ball bearings (BB's) and also using CIRS phantoms with small (160 to 320 micron) calcifications. Scans with the BB's were run with the BB's compressed to the detector, and also suspended above the detector from a tripod to observe the effects of detector as well as tube motion on the image quality. Variables in the tests included the number of view angles (8 or 11), the detector position (CC or MLO [both left and right]), the angular range (40 or 50 degrees), height of the gantry (detector 1 m up or 1.25 m), whether the gantry height adjustment mechanism was free or bolted in place, and direction of tube motion. It was determined

that, as expected, system vibration was least with the detector low and bolted, and for MLO scans, with the tube rising against gravity.

### **3. System Validation**

#### **3.a. Vibration Testing**

An accelerometer was used to measure the vibration characteristics of the tomosynthesis prototype, both before and after the mechanical modifications described in Section 2d were made. The intent of the original measurements was to determine the stiffness and the natural frequencies of the system and to determine which modifications would provide the greatest improvement. The measurements after the modifications characterize the extent of the improvement from a strictly mechanical point of view. The impact of vibration on tomosynthesis image quality is characterized independently, as described in the next section.

Tests of the original DMR system, before the tomosynthesis modifications, showed natural frequencies in the range of 3.25 to 5.25 Hz in the Cranio Caudal (CC) position, and between 4.375 and 9.375 Hz in the Mediolateral (ML) position. For excitation at the bottom of the tube arm, the tube moved 0.73 mm/N for the lowest natural frequencies (below 4 Hz).

After the mechanical modifications for tomosynthesis were made, the lowest natural frequency is increased to 6.75 to 7.5 Hz in either CC or ML position, for an increase (improvement) of over a factor of 2 in lowest natural frequency. At 6.75 Hz, the tube moved 0.08 mm/N when excited at the bottom of the tube arm, or an improvement of nearly a factor of 10. The reinforced system is therefore approximately 10 times stiffer than the original configuration. These measurements confirm a significant improvement in vibration resistance due to the mechanical modifications made to the system, and suggest that additional benefits due to further modifications to this existing mechanical platform (not originally designed with tomosynthesis motion in mind) will be exceedingly difficult to achieve.

#### **3.b. Image Quality Testing**

As mentioned earlier, the image quality testing we performed was mostly concerned with quantifying vibration and its impact on image quality. A first analysis of the system characteristics revealed that the part of the vibration which has an impact on the image quality, can be separated into two different components.

- One component concerns the subassembly consisting of tube and detector including the connecting mechanical structure between these two. If there is vibration within this subassembly, i.e., if the tube moves relative to the detector, then the imaged

structures will appear blurred in the acquired image. Note that this is true even in the case when the object is stationary with respect to the detector, e.g., for a phantom which is “clamped” between compression paddle and detector cover.

- The second component of the vibration relates to a motion of the whole subassembly (consisting of tube and detector, plus the connecting mechanical structure), and is of importance because the patient, even though compressed, will not be completely “coupled” to the system.

The first component of the vibration was quantified by inserting a BB into a Styrofoam block, and then clamping the block between compression paddle and detector cover. The results of this test showed virtually no loss in image quality with respect to a standard projection radiograph. In addition, these results were excellent, independent of the specific scan geometry, and independent of the specific mechanical setup of the system. More specifically, virtually all measurement runs showed blur values smaller than 1, with the majority even being smaller than 0.9.

To measure the second component of the vibration, the same Styrofoam block was “suspended” between compression paddle and detector, without being in direct contact with the system. The first results with this test showed a relatively strong blur, with the worst cases reaching values between 3.0 and 4.0. In addition, these results depended strongly on the specific scanplan and the scandirection used, the position of the considered image within the scan sequence, as well as some of the mechanical system components.

After a number of mechanical modifications to the system, installation of a new ballscrew (see Section 2.d), and selection of specific restrictions concerning the used scanplans and configurations (for example, all MLO scans are to be performed such that the tube movement is performed “against gravity”), this component of the vibration was significantly reduced. From our analysis it can be seen that this vibration component is still larger than the first vibration component, but it is in such a range that the image quality is only slightly impacted.

Specifically, the last tests before shipment of the prototype system as well as the first tests after installation of the system at MGH indicated vibration values of 1.1 or less for 7 or more images within a tomosynthesis scan, with maximum values between 1.3 and 1.4, which were reached by at most 3 images within a scan.

Note that this discussion relates exclusively to the vibration component in scandirection. The component orthogonal to it was virtually vibration-free in all considered cases, with the measured amount of blur typically being smaller than 1.0.

For patient imaging, the situation is a bit more complicated. In this case the breast is compressed, that is, the skin which is in contact with either compression paddle or detector cover, as well as some portions of the tissue directly under the skin can be

considered to be stationary with respect to the detector/tube assembly, and the imaging of these regions of the breast will be governed by the first component of vibration. Interior regions of the breast, in particular close to the chest wall, will also undergo a vibration of the second type, although at this point it is not clear how strong this impact will be. Obviously, the measured second vibration component from our vibration tests represents an upper bound for the observed blur when imaging patients. However, the results may also be far better, due to the compression of the breast.

To further evaluate the system vibration and its impact on image quality when imaging patients, measurements were made at MGH using a non-rigid "gel-phantom" used for biopsies/stereotaxy, with a BB inserted into the gel. The blur of the edge of the BB was compared in a stationary acquisition and in a tomo acquisition. The observed vibration in all experiments was very small for all 11 tomo acquisition positions compared to the stationary acquisition, with no significant impact on image quality. The measurement was repeated with a subject clad in a lead apron leaning against the system, thereby simulating a real patient scenario [1]. The vibration measurements remained essentially unchanged, with the vast majority of measurements being smaller than 1.1, and with a single frame indicating a value as high as 1.5. Note that in this scenario the BB was inserted into the phantom, the images were therefore more noisy and had a somewhat structured background, both of which lead to an increase in the measured blur value, which is not due to real blur or vibration.

### **3.c. Reliability Testing**

A preventive maintenance of the system was done by the GE Medical Systems field engineer several weeks before it was sent to MGH. The x-ray tube was replaced as a preventative action. A 5V power supply in the generator was changed in response to system error messages, the DMR console was replaced, and a hand-held x-ray switch was added to the system. Compression force, compressed breast thickness, kV accuracy, and mAs accuracy were measured and verified. The error log on the DMR was carefully examined, and indicated the system was functioning properly.

Reliability testing on the tomosynthesis acquisitions was carried out to verify proper operation. For each test sequence, each tomo technique was repeated 10 times and key timing parameters were recorded. For the 12 techniques available for tomo (6 with 11 view angles and 6 with 8 view angles), this corresponds to 120 tomo acquisitions for tech test sequence. The test sequence was repeated 3 times in its entirety, and several more time to spot check the system, resulting in a total of nearly 500 tomo acquisition sequences in these reliability tests. Testing in the final configuration with parameters based on the timing model discussed in section 2e showed a success rate well in excess of 90%.

Similar testing was carried out for reconstruction of the projections into slice images, the transfer of images (both tomo projections and reconstructions) to the review

workstation, and archive of the data. These tests verified the successful operation of the functions being evaluated.

### **3.d. Phantom & Mastectomy Specimen Images**

The tomosynthesis prototype system was used to acquire images of a new tomosynthesis complex detail phantom developed by Hamburg [11]. The phantom consists of multiple 1 cm thick plates of breast equivalent material and one “object” plate with 16 squares, each of which can contain a structure designed to simulate either a cluster of microcalcifications, a circular mass, or a spiculated mass. The plates of breast equivalent material differ from standard plates in that the glandular and adipose material are swirled together (and not uniformly mixed) to better simulate the complex background in a real mammogram.

A digital mammogram of the phantom, using 5 plates of breast equivalent material along with the object plate is shown in Figure 3.1.a. A tomosynthesis image of a horizontal plane 3 mm above the features of interest is shown in Figure 3.1.b, and a tomosynthesis image of the horizontal plane containing the features is shown in Figure 3.1.c. The features of interest in each of the squares are also labeled in Figure 3.1.c. Note the significantly enhanced detectability in the tomo images. Specifically, the 250 micron diameter microcalcifications are seen in both the standard mammogram and the tomosynthesis image, but the round and spiculated masses are seen only in the tomosynthesis images. Two masses with very low contrast are not seen in the tomo slices. A reader study of feature detectability is in progress [11].

Tomosynthesis images of a mastectomy specimen containing microcalcifications are shown in Figures 3.2.a, 3.2.b, and 3.2.c. For comparison, a digital mammogram of the same mastectomy specimen is shown in Figure 3.2.d. Note the depth information present in the tomo images. The three dimensional distribution of microcalcifications is believed to be a useful indicator of benign versus malignant lesions. [12]

### **3.e. Image Comparison – Shift and Add vs. Filtered Backprojection**

For a set of three mastectomy specimen tomosynthesis images were acquired at MGH, and a full reconstruction of the covered volume was performed using both, shift-and-add and filtered backprojection algorithms. The results were reviewed by Dr. Kopans during a visit to MGH.

The shift-and-add reconstruction exhibited relatively low contrast (which is an inherent side-effect of this reconstruction algorithm), while the out-of-plane artifacts, though clearly present and obvious for several markers of relatively high contrast placed into the imaged volume, did not seem to have a negative impact on the perceived image quality. The low contrast of the shift-and-add reconstruction leads in addition to the effect that we have a wide range of image values for the reconstructed images, mainly as a function of the thickness of the imaged object. This represents a potentially significant

drawback as it requires readjusting the viewing conditions (window-width and window-level) for different subregions of the image.

On the other hand, the filtered backprojection algorithm does not exhibit this problem associated with the dynamic range. Here choosing good display parameters is much easier. The high-pass filtering characteristic of the filtered backprojection which enhances fine-scale structures, minimizes the need for readjusting the display parameters for viewing different subregions of the image, although even here display parameters had to be adjusted to achieve optimal viewing conditions. On the other hand, the high-pass filtering leads to two negative side-effects. First, out-of-plane structures are also enhanced, which was clearly visible from the way the markers appeared in the reconstruction, although no negative impact on image quality was observed for regions well within the volume of the mastectomy specimen. And second, low frequency content of the images, which may be important for locating masses is to some extent suppressed. In addition, filtered backprojection reconstructed images showed a more grainy structure.

Overall, it was noted that both reconstruction methods showed clearly the benefit of having "volumetric information", in terms of having an additional "depth component" which is not present in standard mammograms. As an additional result of the image review it was noted that, given the images acquired with the present tomosynthesis system (with a limited angular range), a slice separation of 1mm for the reconstructed volume is sufficient to capture even small calcifications and other fine-scale details. When comparing reconstructions performed with a slice separation of 0.1 mm it was observed that sets of several adjacent slices showed virtually no difference, i.e., no information was lost when viewing only slices with a separation of 1mm. In general, Dr. Kopans showed a preference for the filtered backprojection images over the shift and add images.

For comparison, Figures 3.3a, 3.3b, and 3.3c show the shift and add reconstructions of the same slices of the mastectomy specimen reconstructed with filtered backprojects in Figures 3.2a, 3.2b, and 3.2c.

#### **4. System Installation at Massachusetts General Hospital**

##### **4.a. Installation and Validation**

The tomosynthesis prototype system was installed at Massachusetts General Hospital on August 9 and 10, 2000. The complete system (except for the Image Review Workstation) was shipped by air suspension moving van from Schenectady, NY, to Boston. The Full Field Digital Mammography system at MGH was de-installed and returned to GE CRD. The system was successfully brought up, and initial digital tomosynthesis images were acquired with the system at MGH on August 10, 2000.

More comprehensive system validation testing was carried out at MGH on September 5 - 7, 2000. Testing consisted of acquiring tomosynthesis images of phantoms at all the x-ray techniques available on the system for tomosynthesis. Scans were acquired in approximately 35 different imaging configurations, with the only significant failure resulting from the operator entering the wrong x-ray parameters on the DMR console. As a result, DMR and tomosynthesis parameters were not matched, and the system "ran out of dose", leaving the last several angular positions of the tomo acquisition without x-rays. A second test of the same configuration with the proper x-ray parameters was successful.

Detailed characterization of the system functional characteristics (dose, linearity, half value layer, collimation, etc.) are described in Appendix 2 [1]. In summary, "the tomosynthesis unit is performing well and is ready for initial patient imaging".

#### **4.b. Operator Training and First Patient**

A training program has been generated based on the User's Manual (Appendix 3). It is expected that training can be completed in two days, based on the hospital personnel's previous experience with the FFDM prototype. Day one will feature an overview of the Manual, several demonstrations of the system on phantoms, and use of the system by GEMS and MGH personnel on phantoms. Day two will consist of MGH personnel using the system with GE-CRD personnel observing and advising if necessary. A GE Medical Systems application specialist is expected to participate in the training.

## **6 Key Research Accomplishments**

**7**

- System vibration identified as a potential cause of image blur
- A program of vibration testing, analysis and reduction has been successfully completed
- A reliability analysis has been completed. Reliability is over 90%
- A standard phantom has been imaged to verify image quality
- A series of three patient datasets were reconstructed by different methods to evaluate image characteristics.
- The clinical feasibility automatic motorized tomosynthesis system has been completed, delivered, and installed at MGH
- The acceptance testing of the clinical feasibility tomosynthesis system is complete
- The human studies protocol is approved and current with the MGH IRB
- Human studies have commenced

## **7. Reportable Outcomes**

- GE CRD has proceeded with a patent application for a derivative mechanism
- Abstract presentation at RSNA 1999 on tomosynthesis system design
- An RSNA Hot topics abstract was submitted for RSNA 2000

## **8. Conclusions**

The feasibility automatic motorized tomosynthesis system has been delivered, installed and acceptance tested at MGH. .

GE interpreted recent FDA guidance as requiring the design and installation of an articulating collimator. GE CRD has designed and installed this subsystem

Commencement of clinical feasibility and validation testing is unavoidably delayed by approximately one year from plan due to unanticipated development issues at GE CRD. If needed, an application for no-cost extension will be filed to permit completion.

We are now in position to evaluate tomosynthesis in the clinical setting. This will permit an understanding of it's clinical potential, and if warranted, the design of a clinical trial.

## 9. References

1. Niklason, L. "Tomosynthesis System Testing", September 6-8, 2000. See Appendix 2.
2. H. Matsuo, A. Iwata, I. Horiba, and N. Suzumura, "Three-dimensional image reconstruction by digital tomo-synthesis using inverse filtering," *IEEE Trans. Med. Imaging*, vol. 12, No. 2, pp. 307-313, 1993.
3. G. Roy, R. Kruger, B. Yih, and P. Del Rio, " Selective plane removal in limited angle tomographic imaging," *Med. Phys.* vol. 12, pp. 65-70, 1985.
4. D. Chakraborty, M. Yester, G. Barnes, and A. Lakshminarayanan, "Self-masking subtraction tomosynthesis," *Radiology*, vol. 150, pp. 225-229, 1984.
5. P. Edholm and L. Quiding, "Reduction of linear blurring in tomography," *Acta Radiol*, vol.10, pp. 441-447, 1970.
6. U. Ruttimann, R. Groenhuis, and R. Webber, "Restoration of digital multiplane tomosynthesis by a constrained iteration method," *IEEE Trans. Med. Imaging.*, vol. MI-3, pp.141-148, 1984.
7. S. Kawata and J. Sklansky, "Elimination of nonpivotal plane images from X-ray motion tomograms," *IEEE Trans. Med. Imaging*, vol. 4, No. 3, pp.153—159, 1985.
8. S. Kawata and O. Nalcioglu, "Constrained iterative reconstruction by conjugate gradient method," *IEEE Trans. Med. Imaging*, vol. MI-4, pp. 65-71, June, 1985.
9. Z. Kolitsi, G. Panayiotakis, and N. Pallikarakis, "A methods for selective removal of out-of-plane structure in digital tomosynthesis," *Med. Phys.*, vol.20, no. 1, pp.47-50, 1993.
10. Kopans, DB, "Development and Clinical Evaluation of Tomosynthesis for Digital Mammography", Grant DAMD17-98-1-8109, Annual Report, January, 2000.
11. Hamburg, Leena, "Tomosynthesis Breast Imaging: Early Detection and Characterization of Breast Cancer, DAMD17-97-1-7144, Final Report.
12. Conant EF, Maidment AD, Albert M, Piccoli CW, Nussbaum SA, McCue PA. Small-Field-of-View Digital Imaging of Breast Calcifications: Methods to Improve Diagnostic Specificity, *Radiology* 1996; 201(P): 369 (abstract).

## 10. Figures

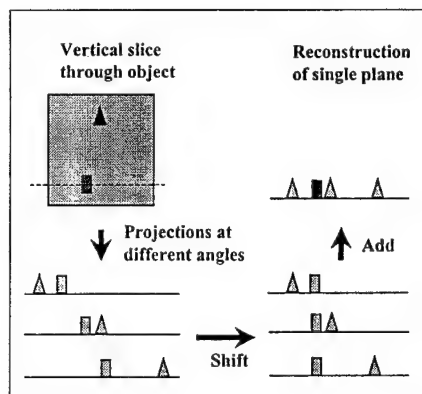


Figure 2.1: Illustration of the shift-and-add reconstruction algorithm, for projections from three different angles.

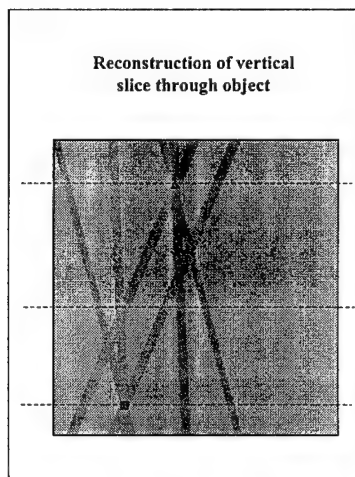


Figure 2.2: Illustration of the "star-shaped" point spread function associated with the shift-and-add reconstruction algorithm. In this example we consider two small point-like structures, and projections from three angles.

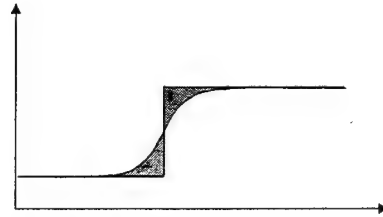
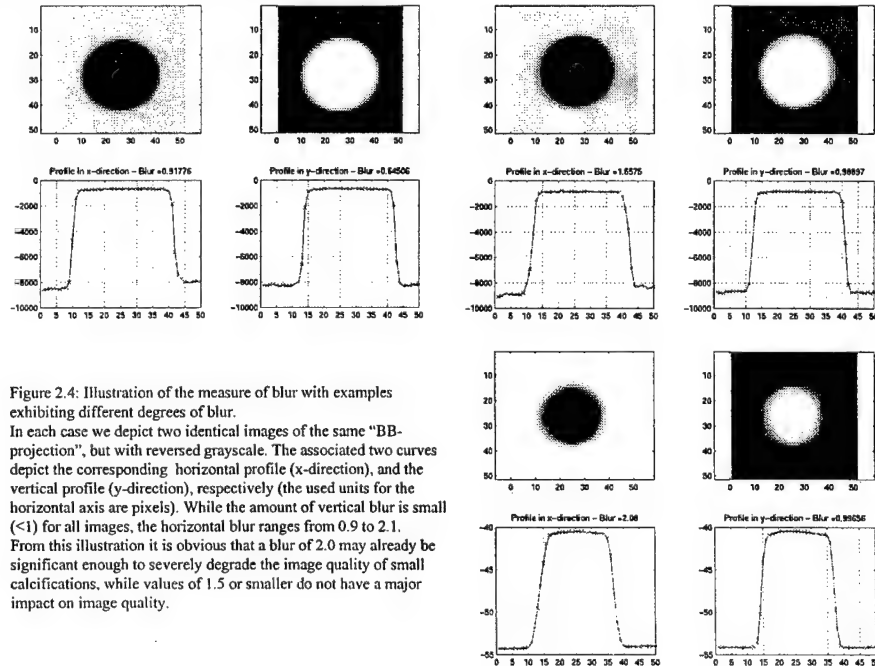


Figure 2.3: Illustration of the approach used to quantify blur/vibration. Ideally the grayscale profile across an edge will be a step function, but due to blurring we observe a "smooth version" of the step function. In this example, the step function is an optimal approximation of the considered "blurred" edge in the sense that it minimizes the shaded area between both curves. After normalization of "height" of the step, the shaded area is the measure used to quantify the amount of blurring.



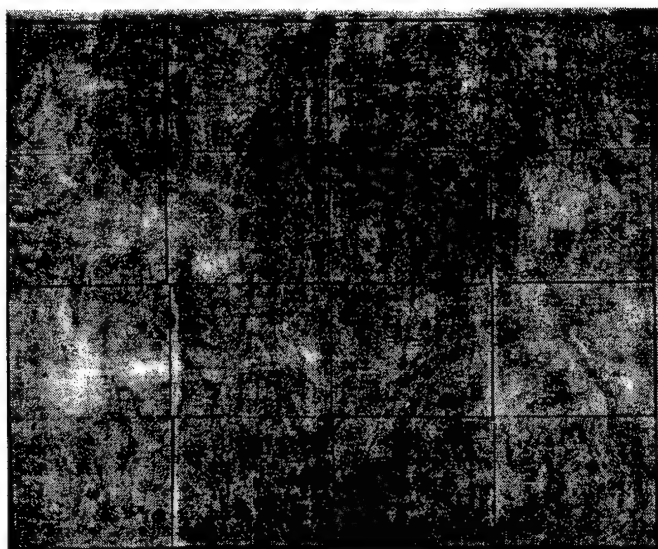


Figure 3.1a. Digital Mammogram of Complex Detail Phantom.  
Note the microcalcifications visible in the upper right square.

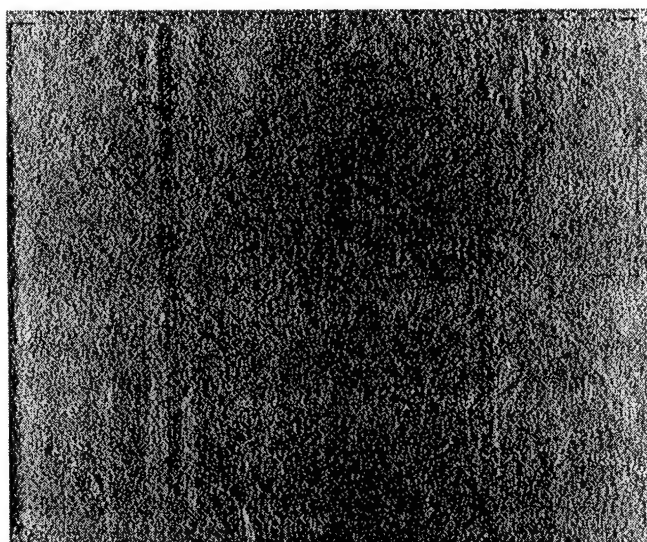


Figure 3.1b. Tomosynthesis Slice of Complex Detail Phantom,  
3 mm above the features of interest.

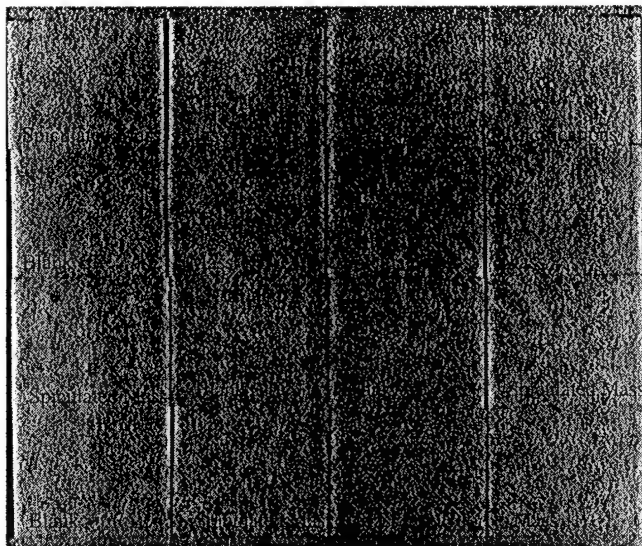


Figure 3.1c. Tomosynthesis Slice of Complex Detail Phantom, through the features of interest. Note the improved detectability of the various features compared to the standard mammogram.

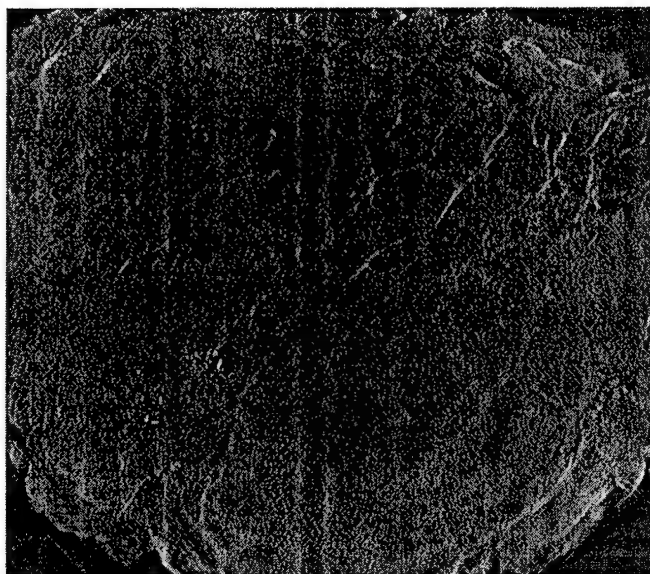


Figure 3.2a. Filtered backprojection reconstruction of a slice through mastectomy specimen 10047, showing microcalcifications. Height = 2.1 cm.

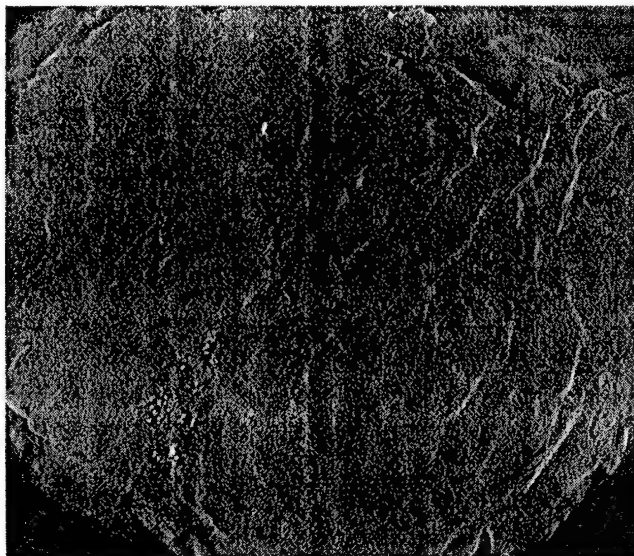


Figure 3.2b. Filtered backprojection reconstruction of a slice through mastectomy specimen 10047, showing microcalcifications. Height = 2.4 cm.

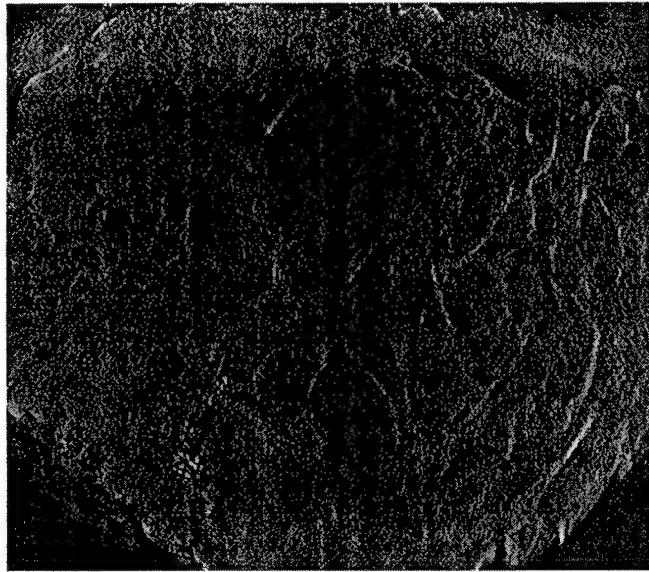


Figure 3.2c. Filtered backprojection reconstruction of a slice through mastectomy specimen 10047, showing microcalcifications. Height = 2.7 cm.

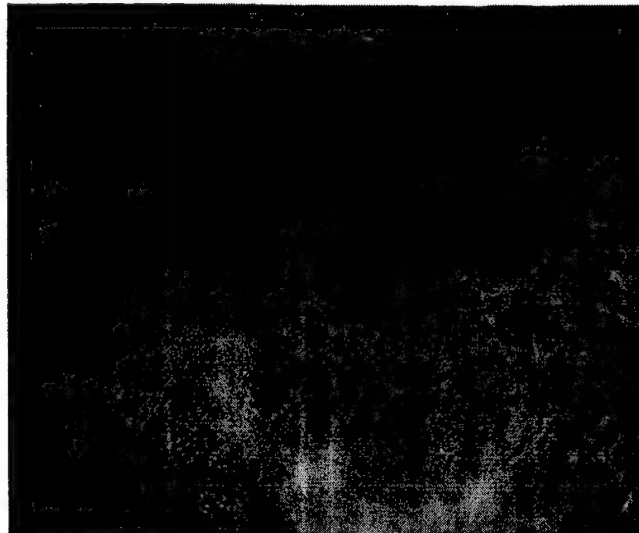


Figure 3.2d. Digital mammogram of mastectomy specimen 10047, showing microcalcifications.

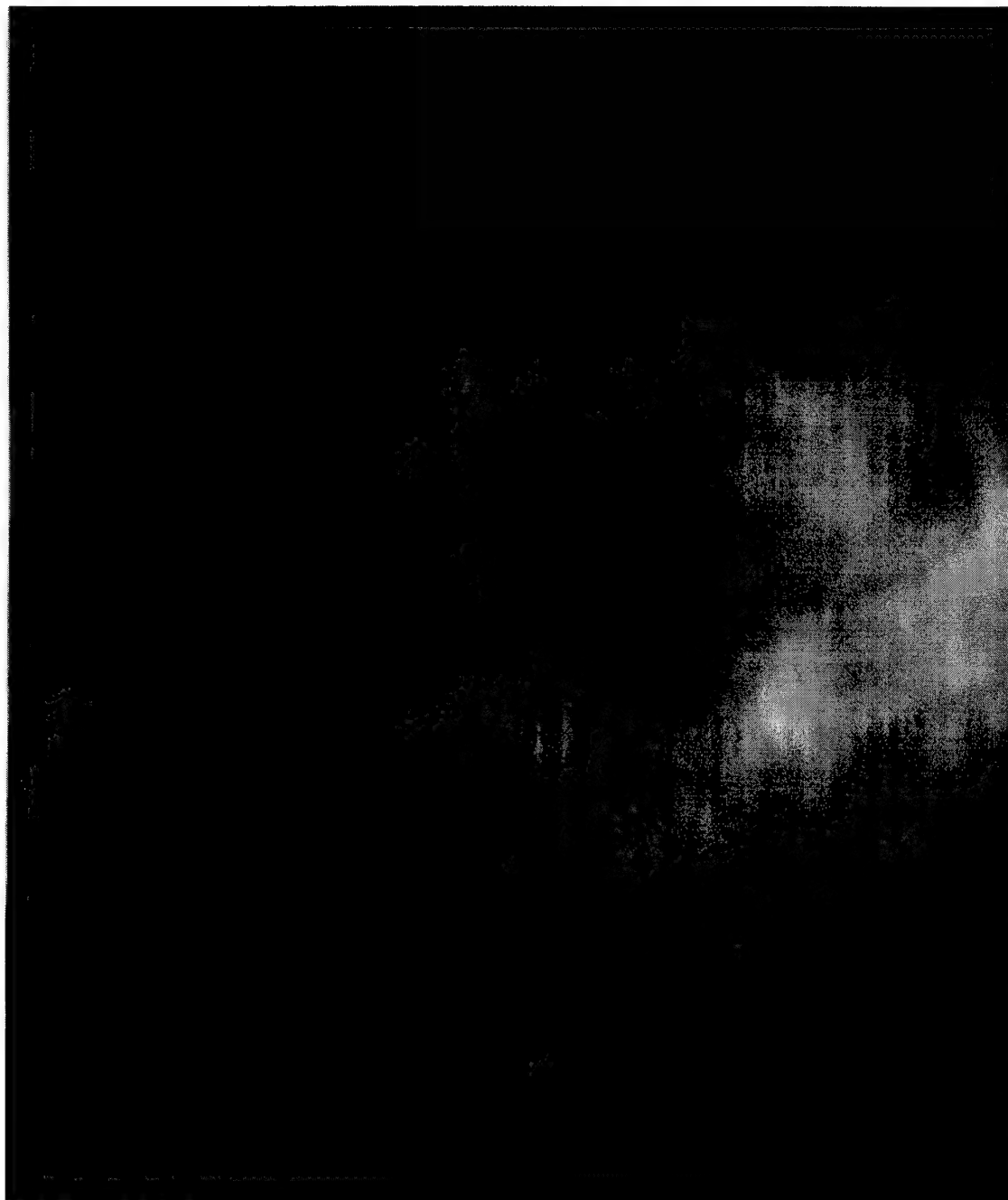


Figure 3.3a. Shift and add reconstruction of a slice through mastectomy specimen 10047, showing microcalcifications. Height = 2.1 cm.



Figure 3.3b. Shift and add reconstruction of a slice through mastectomy specimen 10047, showing microcalcifications. Height = 2.4 cm.

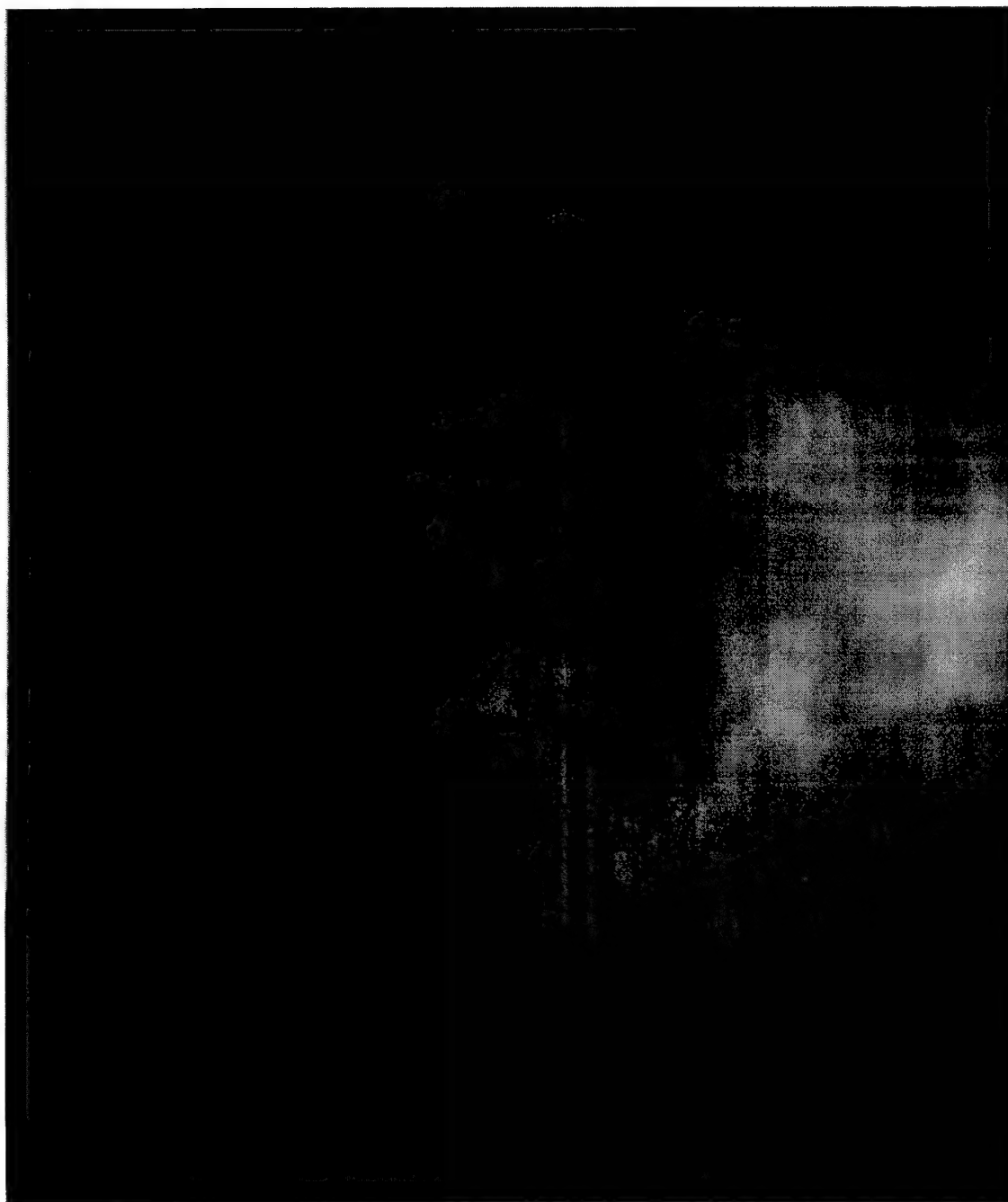


Figure 3.3c. Shift and add reconstruction of a slice through mastectomy specimen 10047, showing microcalcifications. Height = 2.7 cm.

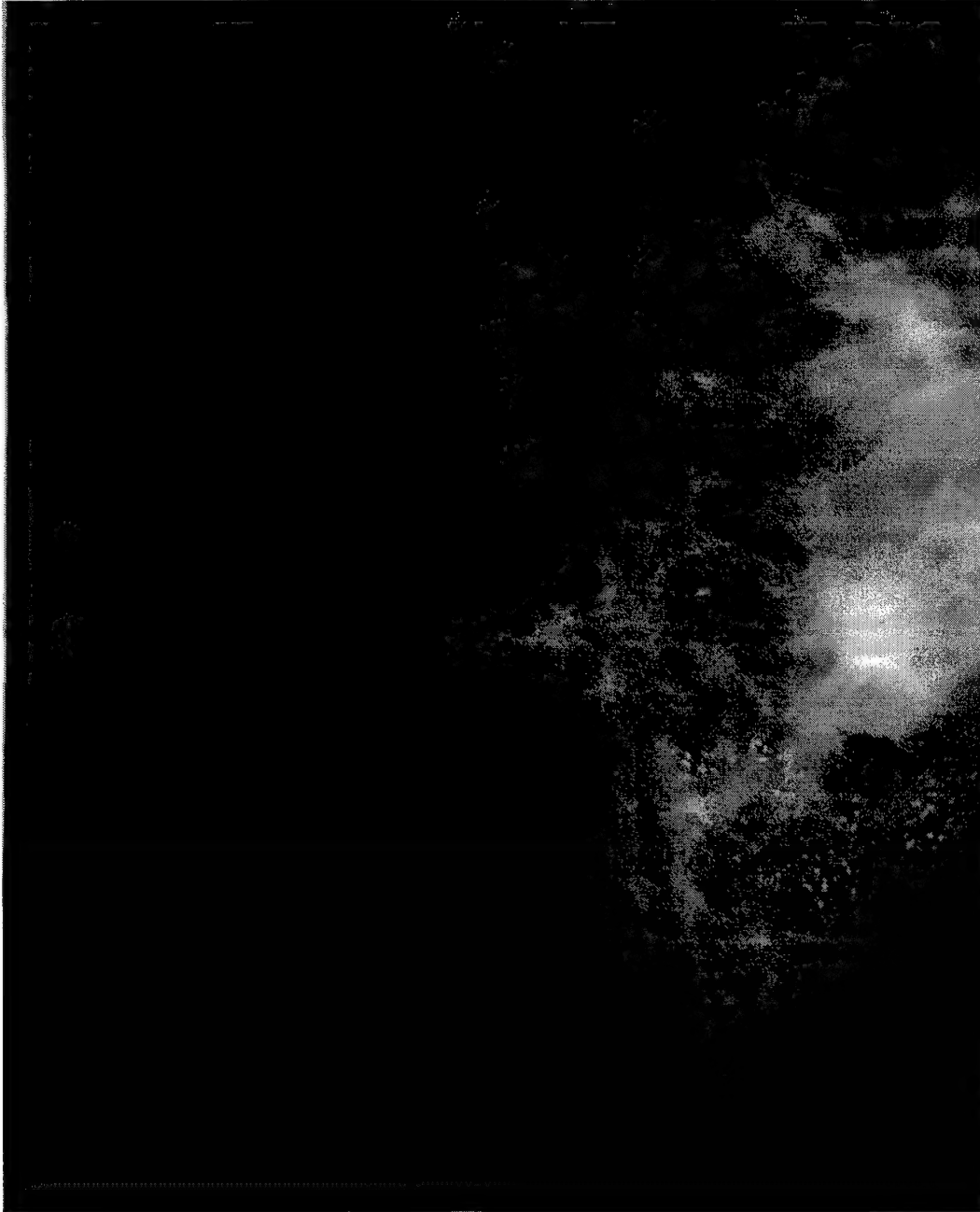


Figure 3.2d. Digital mammogram of mastectomy specimen 10047, showing microcalcifications.

## **11. APPENDICIES**

### **Appendix 1: GE Summer Intern Report on "Out-of-Plane Structure Removal in Tomosynthesis" :**



# Out-of-plane Structure Removal in Tomosynthesis

Lei Ying  
Summer intern  
IEL GE CR&D

August 17, 2000



## Outline

- **Introduction to tomosynthesis**
  - Shift-and-add reconstruction
  - Problem: out-of-plane structures
- **Algorithms**
  - Iterative method
  - Unsharp-masking
  - Blurring subtraction
  - Inverse filtering
- **Results**
  - Simulated data
  - Phantom data
- **Conclusions**

## Constrained Iterative Method (Ruttimann)

### Motivation

Iteration: Update intermediate result by (estimate of) error

### Algorithm

Projection and back-projection (shift-and-add) linear operator  $H$ :  $T = Hf$

Include prior knowledge by nonlinear constraint operator  $C$ :  $f = Cf$

- Initialization:  $f^0 = T$

- Iteration:  $f^{k+1} = Cf^k + \lambda H(f - Cf^k)$

For convergence:  $0 \leq \lambda \leq 2/N$ , where  $N$  is the number of planes

### Advantage:

- Converges to a solution of "projection equation"

### Drawbacks

- Solution is not unique
- Acts on whole reconstructed volume, i.e., computationally intensive

## Blurring Subtraction (Kolitsi)

### Motivation:

Minimize out-of-plane structures by subtracting contribution from neighboring slices

### Algorithm:

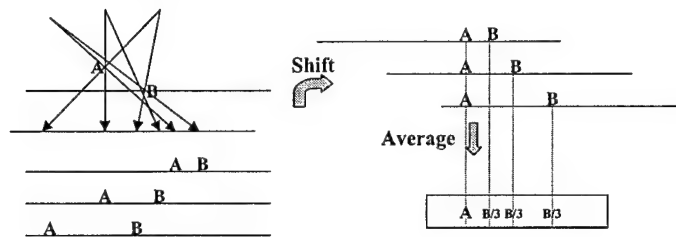
- Reproduce the "artifact image" resulting from out-of-plane structure (by using neighboring slices from shift-and-add reconstruction)
- Subtract "artifact image" from the initially reconstructed image

### Drawbacks:

- Computational complexity increases with number of slices used to compute "artifact image"
- Does not converge, i.e., cannot be used iteratively

## Introduction to Tomosynthesis

- Goal: improve detection and characterization of breast cancer
- Image acquisition: projection from different angles
- Tomosynthesis “reconstructs” any plane parallel to the detector
- Shift-and-add is baseline reconstruction algorithm



## Problem

### Out-of-plane Structures

#### What?

- High contrast structures in the imaged object lead to clearly visible artifacts in the reconstructed volume
- Reduced contrast in reconstruction

#### Why?

- Artifacts are an immediate and obvious consequence of the shift-and-add process
- Projection image “smeared back” across the volume to be reconstructed

## Unsharp-Masking

### Motivation:

- The already blurred out-of-plane structures are unaffected by the additional blurring and can be canceled out of the shift-and-add reconstructed image

### Algorithm:

- Subtract blurred “mask” from shift-and-add reconstruction
- Mask is prepared by low-pass filtering shift-and-add reconstruction
- Low-pass filter is length-21 averaging filter along motion direction of X-ray tube

### Advantages:

- Acts on single reconstructed plane. Computationally efficient
- Simple hardware implementation

### Drawbacks:

- No exact criterion for low-pass filter design
- Does not work well for high frequency component
- Removes low frequency component of in-plane structure

## Inverse Filtering

### Motivation

- Deconvolution in Fourier domain

### Algorithm:

- Assumes parallel beam projection
- Point spread function can be written as

$$h = \sum_{\theta} \sum_Z \delta(x - \Delta Z \tan \hat{\theta}, Z - \Delta Z)$$

$$\hat{\theta} = \tan^{-1}(L \sin \theta / (L \cos \theta + D - Z))$$

- In Fourier domain, the transfer function is

$$H = \sum_{\theta} \sum_Z \exp(-j\omega_x \Delta Z \tan \hat{\theta} - j\omega_z \Delta Z)$$

- Filtering with inverse filter ( $1/H$  for nonzero  $H$ , zero elsewhere)

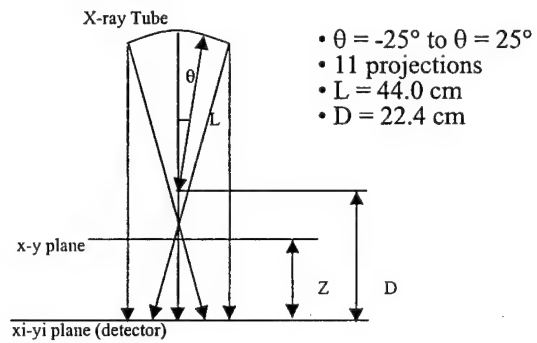
### Advantage:

- One step method, allows to “compute” deconvolution

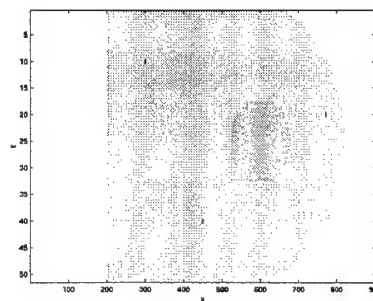
### Drawbacks:

- Parallel-beam assumption does not hold
- Sensitive to noise

## Setup of the System



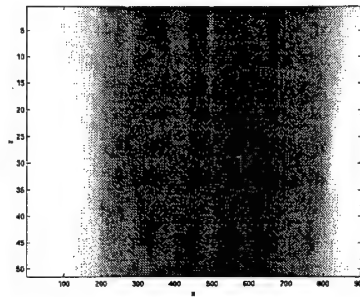
## Simulated Phantom



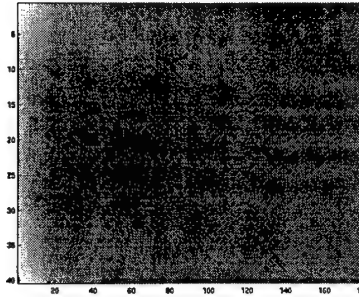
Need to represent different shape and contrast of breast tissue:

- Three dimensional: 121 by 901 by 51 voxels
- 3 microcalcifications, 1 mass.
- All micro calcifications in the same plane as X-ray tube
- Horizontal slice separation 1mm, pixel size 0.1mm

## Conventional shift-and-add

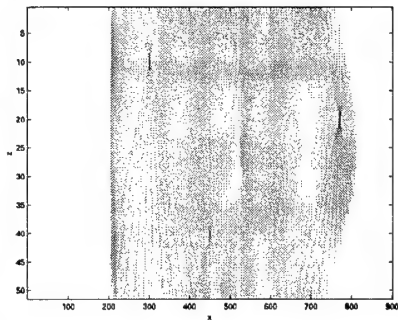


Conventional  
Reconstruction

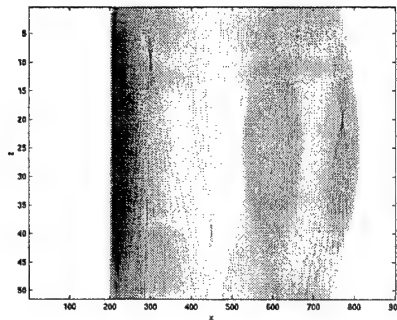


Zoom-In on  
Calcification

## Iteration based approaches

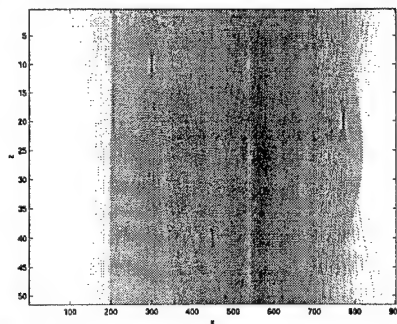


Ruttimann  
(5 iterations,  $=1/N$ )

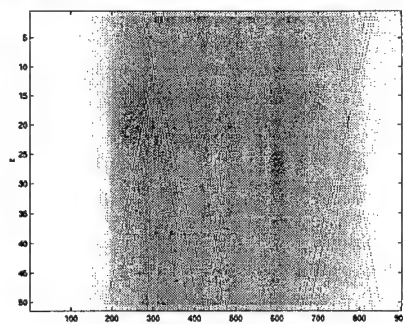


Kolitsi  
(“artifact image” formed by all other planes)

## Filtering based approaches



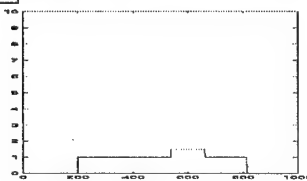
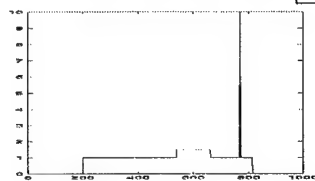
Unsharp-masking  
(length-51 local average)



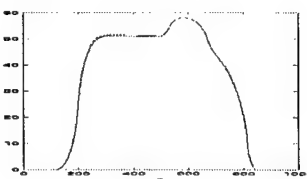
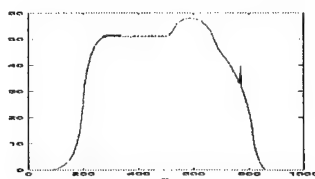
Inverse Filtering  
(filter size 7 by 3)

## Horizontal Profiles Through Simulated Phantom / Reconstruction

Original

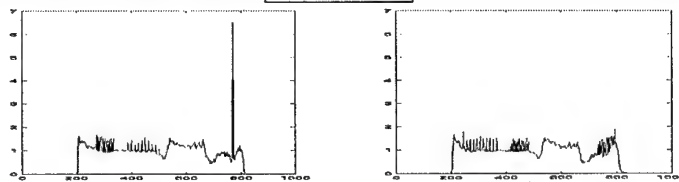


Shift-and-Add

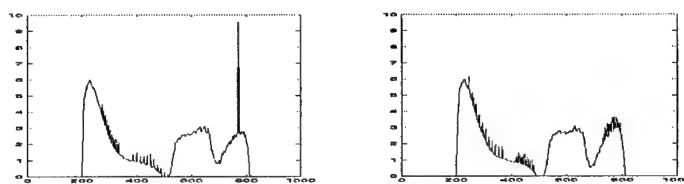


## Horizontal Profiles Through Simulated Phantom / Reconstruction

Ruttimann

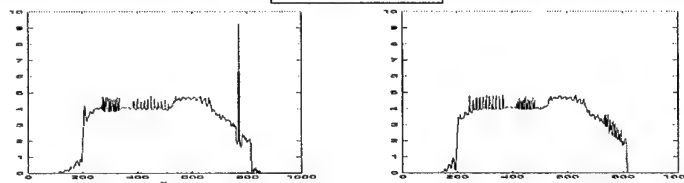


Kolitsi

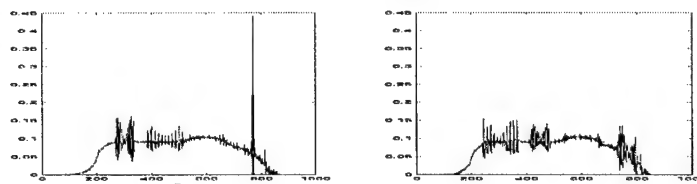


## Horizontal Profiles Through Simulated Phantom / Reconstruction

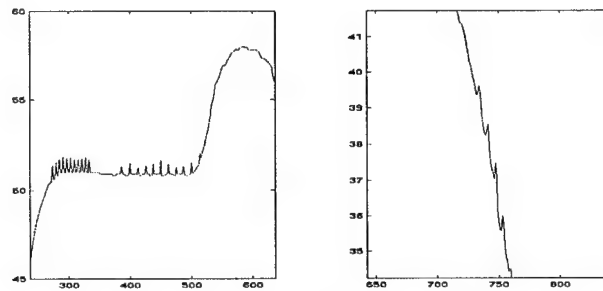
Unsharp-Masking



Inverse Filtering



## Out-of-plane Artifacts

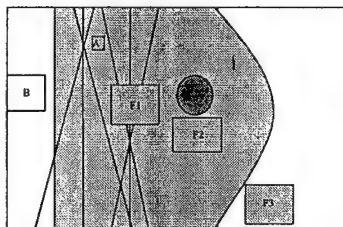


Shift-and-add (zoom)

## Error & Contrast Measurement

- Normalize reconstructed images:
  - Remove constant offset and scaling factor
  - Same "background" within and outside of object
- Error: compute the L1, L2 norm (per pixel) and maximum of the difference between reconstruction and original
- Contrast: compute the L1 norm and maximum of the difference between structure and background.
- L1 norm is defined as  $\|X\|_1 = \sum |x_i|$
- L2 norm is defined as  $\|X\|_F = \sqrt{\sum x_i^2}$
- Maximum:  $\|X\|_\infty = \max |x_i|$

## Regions of Interest for Contrast and Error Measurements



- A, B: Regions used for normalization of images
- F1, F2, F3: Regions used for quantification of artifacts
- Mass & Microcalcifications: Regions used for measurement of contrast

## Artifact and Contrast Measures

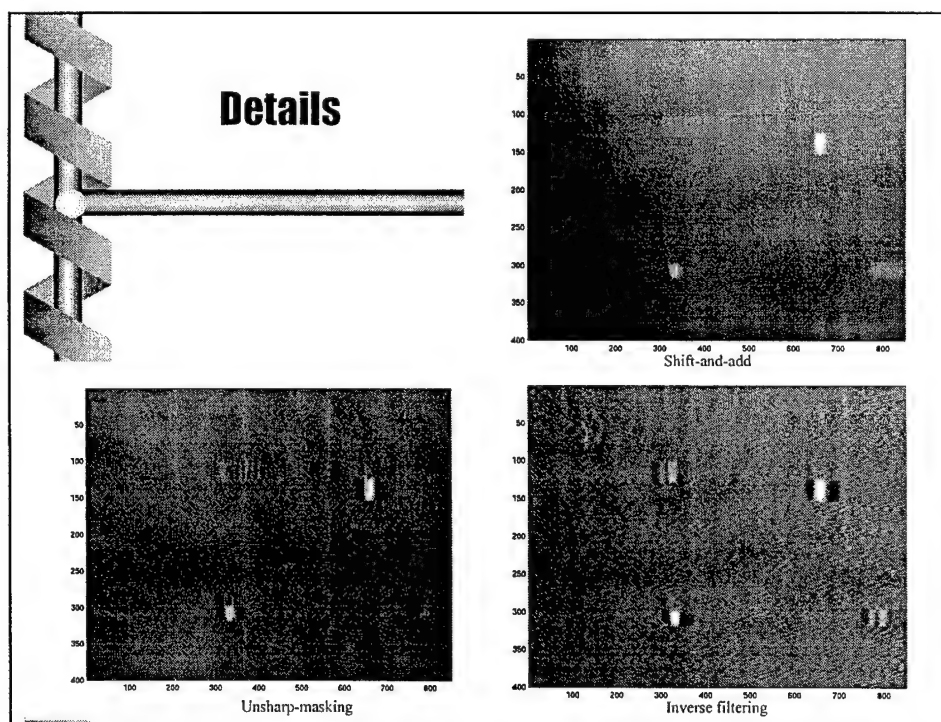
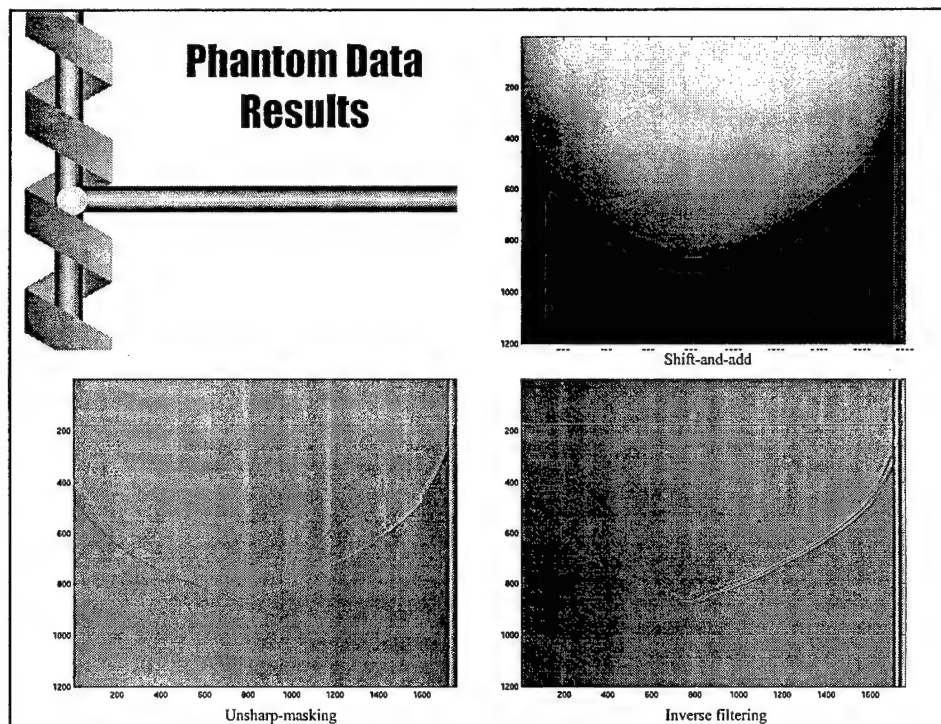
	Artifacts/Errors			Structures/Contrast	
	F1 Microcal	F2 Mass	F3 Boundary	Mass	Microcal
Nominal	0	0	0	0.5	9
Shift-add					
L1	0.0026	0.0849	0.1676	0.1247	0.1355
L2	0.0001	0.0011	0.0036		
max	0.0145	0.1418	0.5488	0.1446	0.1355
Ruttiman					
L1	0.0714	0.0815	0.0044	0.1590	5.0538
L2	0.0020	0.0012	0.0006		
max	0.4703	0.3202	0.8836	0.3962	5.0538
Kolitsi					
L1	0.5560	0.4448	0.0217	0.8031	3.7237
L2	0.0114	0.0061	0.0022		
max	0.9493	0.9472	1.6473	1.0793	3.7237
Mask					
L1	0.0273	0.0850	0.1674	0.1410	2.6426
L2	0.0009	0.0011	0.0036		
max	0.2765	0.1456	0.5990	0.2301	2.6426
InvFill					
L1	0.0536	0.0876	0.1739	0.1246	4.3857
L2	0.0022	0.0012	0.0039		
max	0.6616	0.2616	0.8471	0.2369	4.3857

## Contrast to Artifact Ratio

Contrast-to-Artifact Ratio	Shift-add	Ruttimann	Kolitsi	Mask	InvFilt
Mass (L1)	1.4688	1.9509	1.8055	1.6588	1.4224
Mass (max)	0.8749	0.4713	0.8479	0.9684	0.4763
MicroCal (L1)	52.1154	70.7815	6.6973	96.7985	81.8228
MicroCal (max)	9.3448	11.7027	3.9226	9.5573	6.6289

## Summary of Error measurements

- **Best mass contrast/artifact (L1) ratio:**
  - Ruttimann
  - (Kolitsi)
- **Best mass contrast/artifact (max) ratio:**
  - Unsharp-masking
  - (Shift-and-add)
  - (Kolitsi)
- **Best microcal contrast/artifact ratio:**
  - Ruttimann
  - (Unsharp-masking)
  - (Shift-and-add)
- **Best boundary artifact (L1):**
  - Ruttimann
  - (Kolitsi)
- **Best boundary artifact (max):**
  - Shift-and-add
  - (Unsharp-masking)





## **Conclusion**

---

- **Most methods worked in circular trajectory in original papers. First time derived for the GE prototype system for breast imaging.**
- **No one method performs consistently well in removing out-of-plane artifacts.**

## **Appendix 2: Dr. Niklason's system evaluation:**

### **Tomosynthesis System Testing**

September 6-8, 2000  
Massachusetts General Hospital

#### **General:**

The tomosynthesis unit is performing well and ready for initial patient imaging. The system as currently configured allows imaging with a total tube travel of 40 degrees or 50 degrees and will acquire either 8 or 11 images over this arc. The total imaging time is determined by the exposure time and by the time required to move to the next position. The exposure times are roughly 0.1 seconds and the time to move the tube is currently about 0.6 seconds. Total imaging time for an 11 exposure tomosynthesis exam is approximately 7 seconds, for an 8 exposure exam the total imaging time would be approximately 5 seconds. Whether this will result in significant patient motion during the exam will not be known until we have some experience with actual patient imaging. Anything that can be done to minimize patient motion should be considered, for example, letting the patient hear and perhaps feels the machine noise and vibration during a test run (with no radiation produced) may be beneficial.

Another concern is vibration of the imaging gantry. In the testing, having someone lean against the gantry appeared to reduce the effect of vibration on the image and the system produced images with very little blur. When considering whether to use 8 images or 11 images it is important to keep in mind some of the tradeoffs. In general, I would suggest starting with 11 images since this will allow better "blurring" of out of plane structures and should result in better image quality. Also with 11 images, the vibration issues may be reduced since the tube travels a smaller distance between exposures (this is generally true but not always). The reason for trying 8 images would be to shorten total imaging time if patient motion becomes a significant factor in image quality. There are other issues concerning noise but the primary reasons for choosing 8 or 11 images are listed above.

Image quality as a function of patient radiation dose is another factor to consider. The radiation dose issues are discussed in detail in the report. Based on the phantom images, I would suggest we start patient imaging at about 50% higher dose than a normal mammogram and then determine if the image quality is adequate, if so we should try tomosynthesis images at dose levels matched to

the standard mammograms. Technique charts are attached for three levels of dose.

Overall, the system is ready for patient imaging and should produce excellent images.

## **Testing**

### **1. Vibration Testing**

The systems vibration was tested using four scan plans listed below. These scan plans were tested with and without a person leaning against the gantry. The person was wearing a lead apron and used a small lead shield to shield the head and neck. In these tests a small metal sphere approximately 1-2 mm in diameter was placed in a gel phantom. This phantom was used since it allows some internal vibration in response to system vibration. (Other testing was done by Jeff Eberhard and the GE team using Styrofoam phantoms containing small metal spheres.)

Image file #4 (without person leaning against the system)

Image file #5 (with person leaning against the system)

Scan plans tested:

- 1) 11 images, Rh/Rh, 32 kVp, 110 mAs, 40 degrees, automatic tube motion
- 2) 8 images, Rh/Rh, 30 kVp, 100 mAs, 40 degrees, automatic tube motion
- 3) 11 images, Rh/Rh, 32 kVp, 110 mAs, 50 degrees, automatic tube motion
- 4) 11 images, Rh/Rh, 32 kVp, 110 mAs, 50 degrees, asynchronous tube motion

Note: in the case of asynchronous tube motion the tube had time to stop vibration between exposures, thus these images are made without significant vibration.

Results: Observing the blur at the boundary of the metal sphere there appeared to be a small amount of blur, (approximately 50 microns) without a person leaning on the detector. When a person was present the blur was nearly gone. The 8 image set was noisy.

### **2. Image Gain and Noise**

Testing of the system gain and image noise was accomplished by changing the system gain and looking at the result of this change on image signal-to-noise ratio (SNR).

Results: Individual images at the lower gain setting and the lowest dose levels had pixel values of 90-100. These improved significantly when the higher gain was used. A 50% increase in system gain resulted in a 14% improvement in SNR. This higher gain setting will be used for the rest of the tomosynthesis experiments. (Note: the lowest dose levels were for the 26 kVp, 11 images, 140 mAs, 50 degree scan plan)

### 3. Uniformity

The system has a uniformity test in the QC tools but this did not work. I tested the image uniformity manually. These tests were made using the grid after calibration of all three target/filter combinations. For Mo/Mo and Mo/Rh 1" of Lucite was used as a phantom, for Rh/Rh 2" of Lucite was used.

Regions tested

Region	Row	Column
1	300	200
2	1052	200
3	1900	200
4	300	1000
5	1052	1000
6	1900	1000
reference	1052	700

These coordinates are for the upper left-hand corner of each region of interest. Each region was 200 x 200 pixels.

Uniformity was measured by comparing the signal-to-noise ratio of the 7 regions shown above. These regions included the corners, chest wall and anterior edges and center. All of the region's SNR should be within 20% of the center region (reference region).

Moly/Moly, Grid, 1" of Lucite, 26 kVp

Region	Mean	SD	SNR	% SNR diff/ref
1	4334	32.8	132.1	0.56
2	4331	32.2	134.5	2.37
3	4332	35.4	122.4	-6.87
4	4341	34.3	126.6	-3.68

5	4335	33.9	127.9	-2.68
6	4335	35.6	121.8	-7.32
reference	4336	33	131.4	

### **Moly/Rh, Grid, 1" of Lucite, 28 kVp**

Region	Mean	SD	SNR	% SNR diff/ref
1	9400	46.5	202.2	-1.79
2	9403	44.2	212.7	3.35
3	9410	48.2	195.2	-5.16
4	9409	47.6	197.7	-3.97
5	9407	46.6	201.9	-1.93
6	9411	49.2	191.3	-7.07
reference	9407	45.7	205.8	

### **Rh/Rh, Grid, 2" of Lucite, 30 kVp**

Region	Mean	SD	SNR	% SNR diff/ref
1	8762	60.8	144.1	-16.47
2	8691	54.3	160.1	-7.23
3	8783	65.6	133.9	-22.40
4	8756	56.8	154.2	-10.65
5	8671	52.9	163.9	-5.00
6	8759	61.8	141.7	-17.85
reference	8644	50.1	172.5	

Note: on this image one corner is out of spec.

#### **4. Bad Pixels**

The system has 3476 bad pixels as determined using the bad pixel calibration. I made bad pixel and gain images at 50% of the mAs indicated due to potential saturation. These values will be changed by GE to the lower values.

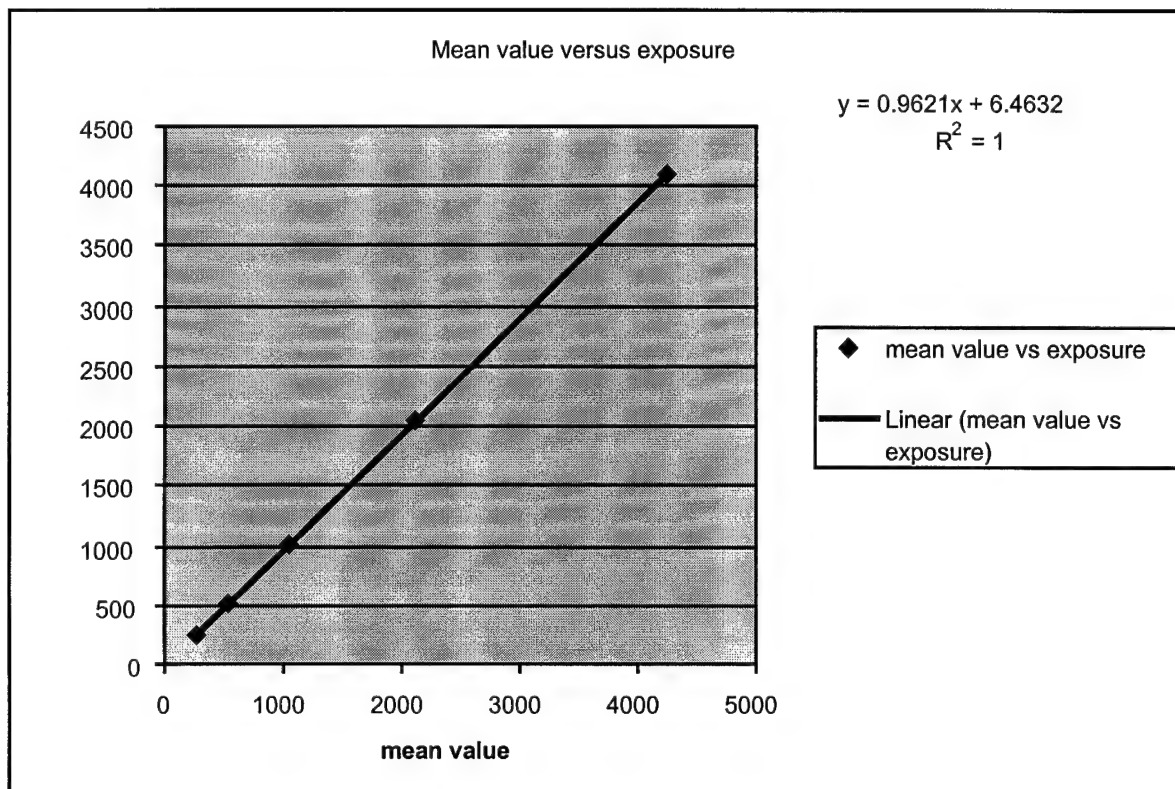
#### **5. Linearity and Reproducibility**

The system linearity was measured by making exposures from 25 to 400 mAs and recording the mean and standard deviation for each region. Two images were made at each mAs and for 100 mAs 5 images were recorded to measure

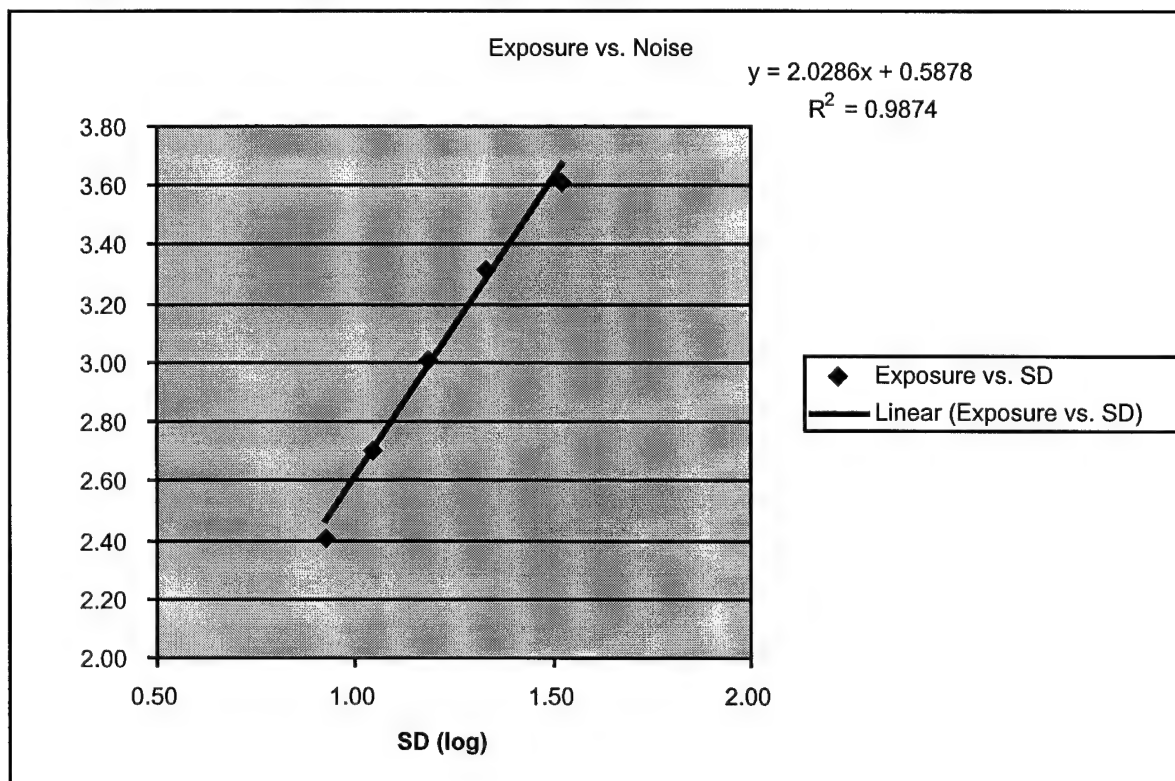
the reproducibility. Results are shown for Moly/Moly, similar results were obtained for Rh/Rh and Mo/Rh. Region of interest of 100 x 100 pixels was used in the center of the image (1 cm squared). In addition the exposure was measured by placing an ion chamber on top of the 2" Lucite block. Technique used was 26 kVp.

mAs	exposure (mR)	mean	SD	SNR
25	252	262	8.45	31.01
50	507	527	11.09	47.52
100	1020	1053	15.15	69.50
100	1021	1053	15.18	69.37
100	1021	1053	15.32	68.73
100	1021	1053	15.32	68.73
100	1021	1053	15.28	68.91
200	2047	2106	21.29	98.92
400	4090	4252	33.27	127.80

note the 400 mAs exposure was split into two separate exposures



Limit less than 1% deviation form best fit (pass)



Limit is R greater than 0.9 (pass)

## Reproducibility

Coefficient of variation for the five exposures made at 100 mAs (SD/mean)

Exposure Variability	COV=0.0004
Pixel Value Variability	COV=0.0000

Limit 0.05

## 6. Tube Leakage and receptor transmission

Limit less than 100 mR/hour at 1 meter using maximum technique. Pass  
Transmission through receptor- Tested at full range of motion pass (+/- 25 degrees)– Pass

Note: For these values I just checked the values made at CRD to validate that they were still correct.

## 7. Image Quality of Tomosynthesis images versus dose

We used a 5 cm complex detail phantom to look at three objects, simulated calcifications, rounded masses and spiculated masses. Techniques and results are shown:

- 1) 11 images, 50 degrees, Mo/Mo, 26 kVp, 140 mAs ( mean value of each image 150, image too noisy) Note: this is lower dose than a standard mammogram.
- 2) 11 images, 50 degrees, Rh/Rh, 28 kVp, 110 mAs ( mean value of each image 350, image OK) This dose is close the that of a standard mammogram.
- 3) 11 images, 50 degrees, Rh/Rh, 32 kVp, 110 mAs ( mean value of each image 710, image very good, very low noise, high dose image)
- 4) 8 images, 40 degrees, Rh/Rh, 28 kVp, 100 mAs ( mean value of each image 410, image good)

At 4 cm we also repeated image 3 which was very good with very low noise.

## 8. Image quality – Non Tomosynthesis images

Images of both the ACR and IDMDG phantom were obtained to look at overall image quality of the detector. These images were made without tomosynthesis.

#### ACR phantom

##### Techniques

Mo/Mo, 26 kVp, 110 mAs, Grid

Mo/Rh, 27 kVp, 71 mAs, Grid

Rh/Rh, 28 kVp, 45 mAs, Grid

##### Results

	Mo/Mo	Mo/Rh	Rh/Rh
Specks	4	3.5	4
Fibers	5.5	4.5	4
Masses	5	4	4
Mean background	3150	1212	1620
Mean disk	2680	945	1320

The Mo/Mo technique passes the limits of 5 fibers, 3 specks and 3 masses set by the IDMDG. And all pass the current ACR guidelines. Note the Mo/Rh and Rh/Rh images were obtained at much lower dose than the Mo/Mo images. Dose levels for these images are listed in Section 10.

#### IDMDG Phantom

##### Techniques used;

Mo/Mo 160 mAs, 26 kVp

Mo/Rh, 120 mAs, 28 kVp

Rh/Rh, 100 mAs, 30 kVp

Images in file 9.

##### Results for Mo/Mo images

**Resolution** (low contrast resolution phantom) 5 x 5 lp/mm

**Chest wall dead space** – using this phantom is 1.2 cm, however measured at the detector is 8 mm. The difference is likely due to the position of the focal spots since for the IDMDG phantom the test object is 5 cm above the detector.

**Visibility of stars** (small objects about as large as microcalcifications but containing 5 points) For 5.4 cm region 13 visible, for 2.8 cm region 14 visible.

For both the star points are visible on 5 stars.

**Contrast Index** (Step 8-Step2) =  $30500 - 8970 = 21530$

## **9. Conversion Factor**

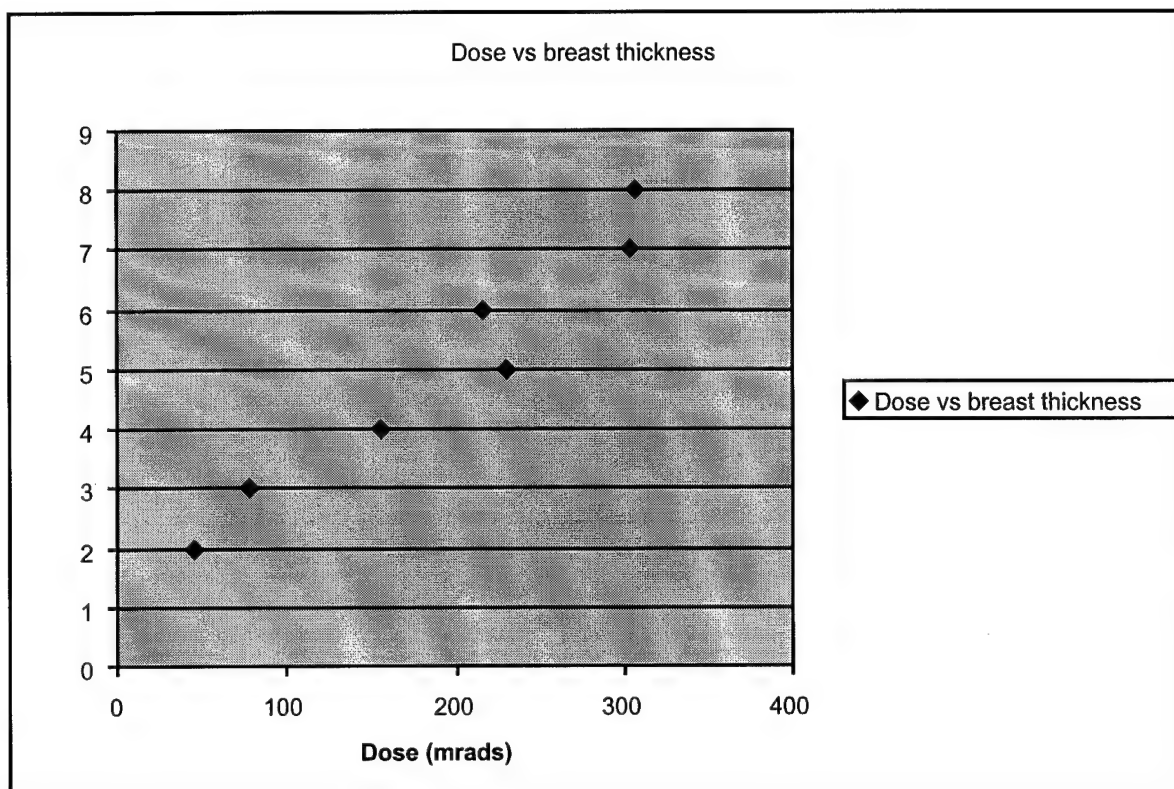
291 (pass)

## 10. Radiation Dose

Radiation dose for the tomosynthesis images is required to be within one to three times that of a single conventional mammogram. This is the range listed in the IRB protocol. To determine the starting point we measured the dose for a range of breast thickness using the film-screen DMR system. These measurements are for a breast composition of 50% gland/ 50% fat.

Contrast mode	Thickness (cm)	Target	Filter	mAs	kVp	Dose (mrads)
	2	Mo	Mo	24	25	46
	3	Mo	Mo	51	25	77
	4	Mo	Mo	102	26	156
	5	Mo	Mo	183	26	230
	6	Mo	Rh	173	27	216
	7	Mo	Rh	173	30	303
	8	Rh	Rh	166	31	306
	ACR	Mo	Mo	116	26	170

Graph of dose vs. breast thickness for a conventional film-screen mammogram



Shown below is the mAs range that will produce radiation doses equal and up to three times that of the conventional mammogram. This table was generated by using the optimum spectra data gathered for the original digital prototype. We have suggested using Rh/Rh for all breast thicknesses based on the optimum spectra data and the need to maximize radiation transmission for a given dose. A higher transmitted x-ray intensity will result from the use of Rh/Rh target/filter combinations. This will produce higher mean pixel values and decrease the chance of significant quantization error. It will also be simpler to start with a single target filter combination. These calculations are based on 50% gland, 50% fat breast composition. Note: the dose from 11 images spread over 50 degrees with a total mAs of 100 is very close to that from a single exposure at 0 degrees of 100 mAs. In previous calculations the dose was slightly less for the 11 views than for the 1 view. For simplicity we will assume that they are equal.

#### Tomosynthesis techniques versus breast thickness

Thickness	Target	Filter	kVp	mAs for matched	mAs for maximum
-----------	--------	--------	-----	-----------------	-----------------

(cm)				dose	dose
2	Rh	Rh	25	22	67
3	Rh	Rh	25	47	142
4	Rh	Rh	26	97	291
5	Rh	Rh	28	121	348
6	Rh	Rh	30	96	288
7	Rh	Rh	31	134	403
8	Rh	Rh	32	133	399

To decide at what dose level to operate may take some clinical experience. As a starting point it is interesting to note that the technique used for technique #2 in the image quality section (section 7 - 5 cm breast thickness) was almost identical in dose to the matched dose technique suggested in the table above. This technique was 28 kVp, Rh/Rh and 110 mAs. The images resulting from this exposure were judged OK, and images of this dose will probably produce good images. The image quality improves as the dose is increased. I have supplied dose tables for matched dose, 50% higher dose and 100% higher dose (compared to a single mammogram). I would suggest we start at approximately 50% higher dose and then try lower or higher depending on the image quality achieved. The final operating point should be based on the clinical image quality.

Note: For the standard digital images (non-tomosynthesis images) use the same techniques shown in the matched dose technique chart. This will result in matched dose with the film-screen mammograms. Attached is a technique chart for these standard digital images.

## 11. Half Value Layer and Radiation Output

All half value layer and radiation output measurements were made with a 25 mAs exposure. Radiation exposure was measured at 4.5 cm above the bucky using a calibrated ion chamber. Shown below are the HVL and radiation output for Moly/Moly, Moly/Rhodium and Rhodium/Rhodium target/filter combinations. These values were used for the radiation dose estimations.

### Moly/Moly

target- filter kVp	MM 24	MM 26	MM 28	MM 30
0 mm Al	156	209	269	336
0.3 mm Al	83.7	118	156	198

0.4 mm Al	69.9	99.2	133	170
0.5 mm Al				147
0.6 mm Al				
0 mm Al	157	209	268	335
HVL (mm Al)	0.34	0.37	0.39	0.41
Radiation Output (mR/mAs)	6.26	8.36	10.74	13.42

Moly/Rh

target- filter	MR	MR	MR	MR
kVp	26	28	30	32
0 mm Al	172	222	280	341
0.3 mm Al				
0.4 mm Al	88.1	119	153	189
0.5 mm Al	76.1	104	134	167
0.6 mm Al				
0 mm Al	172	224	280	341
HVL (mm Al)	0.42	0.45	0.47	0.48
Radiation Output (mR/mAs)	6.88	8.92	11.2	13.64

Rh/Rh

target- filter	RR	RR	RR	RR	RR
kVp	26	28	30	32	35
0 mm Al	182	235	290	353	454
0.3 mm Al					
0.4 mm Al	91.8	124	161		
0.5 mm Al	79.5	108	141	177	238
0.6 mm Al					212
0 mm Al	182	235	289	353	454
HVL (mm Al)	0.41	0.44	0.48	0.50	0.54
Radiation Output	7.28	9.4	11.58	14.12	18.16

(mR/mAs)

These values are all within the specification for HVL from the ACR and MQSA.

Listed below are the radiation doses for digital (non-tomosynthesis) images of the ACR phantom.

**ACR phantom image  
dose**

Target	Filter	kVp	mAs	dose (mrads)
Mo	Mo	26	110	167
Mo	Rh	27	71	121
Rh	Rh	28	45	99

## 12. kVp measurements

These measurements were made to check the accuracy and reproducibility of the kVp. kVp must be within 5% of the nominal value and the coefficient of variation must be less than 0.02.

kVp nominal		24	26	28	30	32	35
kVp measured	1	25	26.8	28.5	30.2	32.1	35
	2		26.9				
	3		26.9				
	4		26.9				
mean kVp			26.9				
SD			0.05				
mean - nominal	1	1	0.9	0.5	0.2	0.1	0
0.05 x nominal	1.2	1.2	1.3	1.4	1.5	1.6	1.75
COV			0.002				

kVp is within limits. Timer reproducibility was also checked and had a COV of 0.002.

## 13. Mechanical Assembly

All of the mechanical systems were checked and found to move adequately. Vertical motion of the gantry is not allowed to reduce vibration. Comments in the beginning of the report address the vibration issues. Patient is not exposed to sharp edges. The accuracy and reproducibility of the compression thickness indicator were checked at 7 dN. Values are listed below:

Actual breast thickness (cm)	Measured breast thickness (cm)
2	2.1
4	4.0
4	4.0
4	4.0
6	6.0

## 14. Focal Spot size

The ACR/MQSA suggest that if the limiting spatial resolution is greater than 13 lp/mm parallel to the anode-cathode direction and greater than 11 lp/mm perpendicular to the anode-cathode direction then a more detailed evaluation is not necessary. Resolution was measured with a screen-film system and the 0.3 mm focal spot. Note; this system does not allow for magnification images.

Nominal focal spot size	0.3 mm	0.3 mm
Target	Moly	Rhodium
Nominal kVp	26	30
mAs	10	7
Limiting resolution parallel a-c	17	16
Limiting resolution perpendicular a-c	18	16

## 15. Collimation

These tests determine if the x-ray field and light field are aligned, if the x-ray field exceeds the dimensions of the detector by more than 2% of the source-to-detector distance (SID), and if the edge of the detector and paddle are properly aligned.

### X-ray field light field alignment

Angle	0 degrees	0 degrees	neg. 25 degrees	neg. 25 degrees	25 degrees	25 degrees
Target	Moly	Rhodium	Moly	Rhodium	Moly	Rhodium
left edge deviation	2	0	1	-4	6	12
right edge deviation	3	-1	8	0	0	0
Sum	5	1	9	4	6	12
Sum as % of SID	0.76	0.15	1.36	0.61	0.91	1.82
Anterior edge	2	4	3	5	1	7

deviation						
Chest wall deviation	1	-5	5	-3	3	-4
Sum	3	9	8	8	4	11
Sum as % of SID	0.45	1.36	1.21	1.21	0.61	1.67

Limit 2% of SID, pass

### **X-ray Field - edge of receptor alignment**

Angle	0	0	neg. 25	neg. 25	25	25
Target	degrees	degrees	degrees	degrees	degrees	degrees
	Moly	Rhodium	Moly	Rhodium	Moly	Rhodium
		m				
left edge deviation	5	2	6	8	9	-15
%SID	0.76	0.30	0.91	1.21	1.36	-2.27
right edge deviation	7	4	2	-8	4	8
%SID	1.06	0.61	0.30	-1.21	0.61	1.21
Anterior edge deviation	4	7	3	2	2	7
%SID	0.61	1.06	0.45	0.30	0.30	1.06
Chest wall deviation	4	2	7	6	6	2
%SID	0.61	0.30	1.06	0.91	0.91	0.30

Limit less than 2%  
outside of detector –  
pass. Note for Rhodium  
at 25 degrees the field is  
inside the detector by  
1.5 cm due to the size of  
the filter.

### **Alignment of chest wall edge and compression paddle**

Angle	0	0	neg. 25	neg. 25	25	25
	degrees	degrees	degrees	degrees	degrees	degrees

Target	Moly	Rhodium	Moly	Rhodium	Moly	Rhodium
		m				
Diff paddle to detector edge	2	3	2	3	2	3
% SID	0.30	0.45	0.30	0.45	0.30	0.45

Limit – must be beyond the detector but less than 1% of SID outside. Pass

**Final Notes:** The system does not have an automatic exposure control or a functioning printer so these were not checked. In addition, the review workstation was not changed in this upgrade and was not evaluated. I would suggest that QC testing be performed on the monitors if these will be used for image review.

## **Appendix 3: FFDM Tomosynthesis Prototype System User's Manual:**

# **Full Field Digital Mammography**

## **Tomosynthesis Prototype**

### **Users Manual**

dms version 3.0

### **Contact Information**

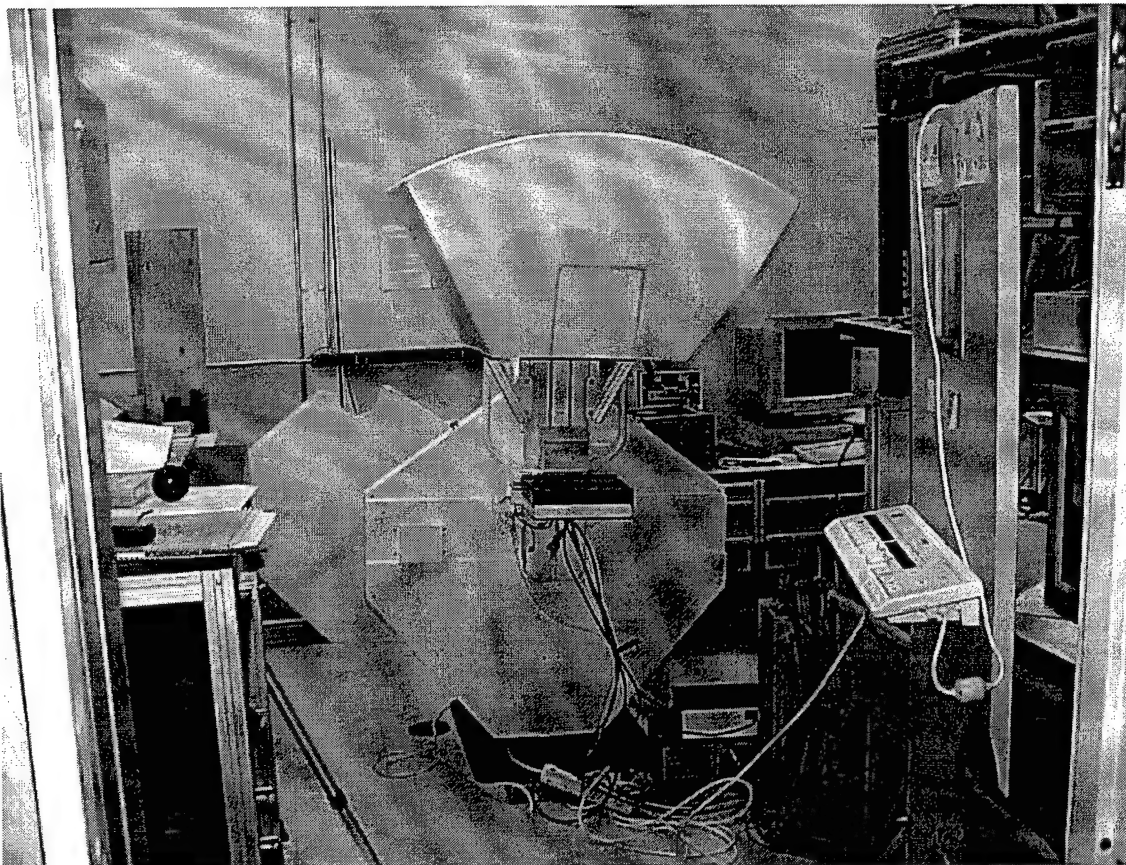
Detector/Hardware	Michael Denvir	518-387-4113
System/General	Jeff Eberhard	518-387-4301

# Chapter 1 Introduction

## Section 1 Presentation

The Tomosynthesis Full Field Digital DMR is the same as the system as described in the Full Field Digital DMR Operator Manual on page 1-1 except that in order to acquire three dimensional information in an exam, magnification is no longer possible, and only the 660 mm SID can be used. Additionally, for Tomo examinations the Bucky grid, used for scatter reduction, must NOT be used, as its design will only pass radiation when the tube is perpendicular to the detector.

## Section 2 Description



### **WARNING**

The system is the same as described in the Full Field Digital DMR Operator Manual except that it incorporates a **high power servo controlled ballscrew drive** to position the x-ray tube relative to the detector, and a second servo controlled drive on the collimator to position it so as to limit radiation to the detector as the tube angle changes. The system has shields around the tube and collimator drive systems to protect the patient and the operator. The system must NOT be used without the shields.

### **WARNING**

The operator must beware of the clearly labeled pinch points at the top of the lower shield, and see that the patient keeps away from them during tomo scans. The DMR gantry **MUST BE BOLTED TO THE FLOOR** to obtain satisfactory image quality.

The X-ray tube will be automatically positioned for an examination, either tomo or non-tomo, or calibration measurements.

## Preparing an Examination

### **Section 1 – Preparing The Equipment**

#### **1-1 Switching on the Equipment**

As for the prototype FFDM system, the detector must be stabilized under power for 30 minutes prior to taking images. The proper order for energizing the equipment is:

- ♦ VME Cage
- ♦ Thermoelectric cooler and FFDM image receptor power supply
- ♦ Computer tapes and disks if computer is off
- ♦ Computer and monitor

The VME cage and detector power supply should be turned off in the reverse order (detector before VME cage), since it may damage the detector to be powered up without the VME cage on.

#### **CAUTION**

The VME cage may be left on for no more than 6 days, as the internal clock on the motion control board will 'wrap' and record confusing data ('W1' problem).

The DMR must be turned on before the motion control system is able to function.

The DMR should be turned OFF at the end of the day's exams, along with the detector power supply. Turning off the DMR will eliminate the possibility of uncontrolled gantry motions.

#### **1-2 DMR Setup**

##### **Spot Size**

For Tomo exams only the LARGE spot size should be used.

##### **Bucky**

For Tomo exams the Bucky **MUST** be removed.

##### **SID**

Only the 660 mm SID is possible with the Tomo system.

##### **RAD Parameters**

For standard (non-tomo) exams refer to page 2-1 in the Full Field Digital DMR Operator Manual.

For Tomo exams, due to the nature of the system, only one combination of Track, kV, mAs, and number of angles in the exam is possible. These are shown in Table T1.

**Table T1 Tomo Rad parameters available**

Number of Angles	Target	Filter	Tube Voltage	MA's
8	Rhodium	Rhodium	28	100
8	Rhodium	Rhodium	30	100
8	Rhodium	Rhodium	32	140
8	Molybdenum	Molybdenum	24	100
8	Molybdenum	Molybdenum	26	125
8	Molybdenum	Molybdenum	28	110
8	Molybdenum	Rhodium	28	110
11	Rhodium	Rhodium	28	110
11	Rhodium	Rhodium	30	110
11	Rhodium	Rhodium	32	110
11	Molybdenum	Molybdenum	24	125
11	Molybdenum	Molybdenum	26	140
11	Molybdenum	Molybdenum	28	140
11	Molybdenum	Rhodium	28	140

**Section 2 Calibration and Quality Control are as described in the Full Field Digital DMR Operator Manual, except that the gantry drive must be operational in order to position the tube perpendicular to the detector and collimator drive must be on to allow irradiation of the entire detector. The system will automatically position the gantry and the collimator. Call CRD if any difficulties occur.**

### **Section 3 Exposure Mode**

Standard Exams: see the Full Field Digital DMR Operator Manual

Tomo Exams: as for standard exams except that as noted above, only certain combinations of exposures are possible, and more compression reduces the three dimensional information obtainable in the exam.

### **Section 4 Clinical Procedure**

#### **4-1 Taking Images**

The software program used on the Sun workstation is named "dms\_tomo", which must be used in order for correct positioning of the tube and its collimator. When an exam is not in progress, the x-ray tube will be positioned so that the operator may easily rotate the gantry for a different view. The system is interlocked so that gantry rotation is not possible unless the tube is in the 'balance' position with the motion control system active.

#### **WARNING**

As before, the **prepa** and **graphe** buttons must be held down during the complete exposure sequence. A software error will occur if they are released prior to the triple 'beep' issued by dms\_tomo after the last exposure is read out, resulting in the loss of the second frame at the final position.

#### **Section 4-4 Problems During Exam**

In addition to the discussion in the FFDM manual, certain problems can arise in conjunction with the motion control system, and its interaction with the rest of dms\_tomo. Table T2 lists the more probable problems and suggested actions to take if they are encountered.

**Table T2 Possible problems during tomo operation**

Problem	Indicated Action
Error Message about communication with the motion control subsystem	Try the operation again. 90+% of the time, the operation will succeed on the second try. If repeated

	failures occur, cycle the power on the VME box (off for ten seconds) and then bring up the TomoTest widget from the main menu. Home both the gantry and collimator. If this is unsuccessful, call CRD.
Error message about motion problems or 'position mismatch' during a scan	Go to the TomoTest widget under the main menu and see if the motion control system is initialized and the motors are on and homed. If not, initialize if necessary and attempt to home if necessary. If unsuccessful, cycle the VME cage power and try to initialize and home. Perform a 'Demo Exam' (see section 3-2-5 in chapter 3). Call CRD if this is not successful.
Inability to release the gantry lock for positioning to another view, especially after an 'Emergency Stop' button has been pressed on the console or on the DMR	The gantry interlock has been coupled to the motion control system so that the gantry cannot be rotated unless the tube is in the 'balance' position, which should be indicated by the green LEDs (light emitting diodes) being energized. If the red LED is lit, go to the TomoTest widget press the 'move to balance position' button. The green LED should soon go on, indicating gantry rotation should be possible. Call CRD if cycling the VME cage power and re-homing are unsuccessful.
Prepa / Graphe buttons released during scan	Reject scan and rerun.
Gantry moves before first exposure	No rerun is necessary if loss of one angle is acceptable (usually 11 angle scan). Call CRD if condition occurs frequently.
'Beeps' end in middle of scan	Try the scan again, after recording the error codes seen on the DMR console into the comment window when the scan is rejected.
Scan ends with E04 'Arm Fatal Failure'	In addition to causes identified in the FFDM manual, E04 will occur if the system has changed characteristics such that all the dose called for by the mAs setting has not been delivered. This data should be fine. Power cycle the DMR before attempting further acquisitions of tomo or normal mammo data. Call CRD if this occurs.
Scans have no exposure in last frame above the noise level.	This is the opposite side of the coin from the E04 too much dose problem. Again, call CRD.

## Positioning the Patient

### **Section 1 Operation of the Tomo System during examinations**

Do not position the patient until the 'Start Capture' button on the 'Start Exam' widget has been pressed. The gantry and collimator drives will position the tube and collimator so that the positioning light correctly illuminates the area to be examined.

### **Section 2 Examinations**

To rotate the detector arm for the desired view, the system must be in the balance position (see table T2 in section 2).

Software

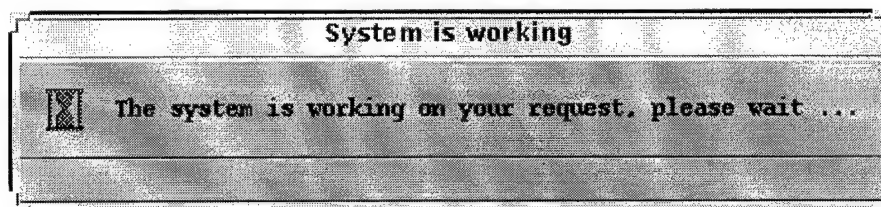
**Section 1 and 2: Same as in FFDM manual.**

### **Section 3 Graphical User Interface – dms\_tomo**

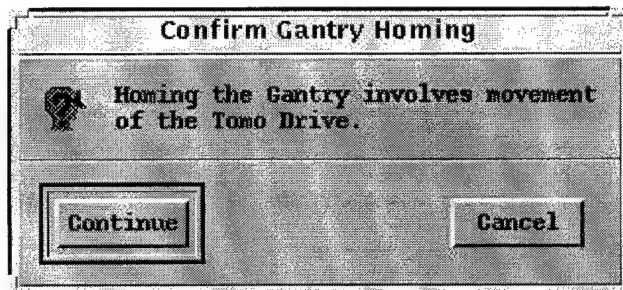
dms\_tomo can be started from any xterm window or from the root window program menu. All widgets have a Help button which will bring up a help widget with all necessary information for its parent widget. Most dms\_tomo widgets are close to corresponding widgets in the dms program for FFDM operation. Differences are noted below, with subsection numbering corresponding to the dms section in the FFDM manual.

#### **3-1 dms\_tomo Main Widget**

When dms\_tomo is invoked, the first things displayed will be the Main Widget with one or more message widgets overlying it relating to the detector panel test automatically invoked. While the panel test is being performed no other operations are possible. This is required since communications to the motion control subsystem will interfere with the panel test. After completion of the panel test, dms\_tomo will initialize the motion control subsystem and request the operation allow the homing operation to proceed if homing is required. Often when dms\_tomo is communicating with the motion control subsystem a 'System is Working' widget will appear

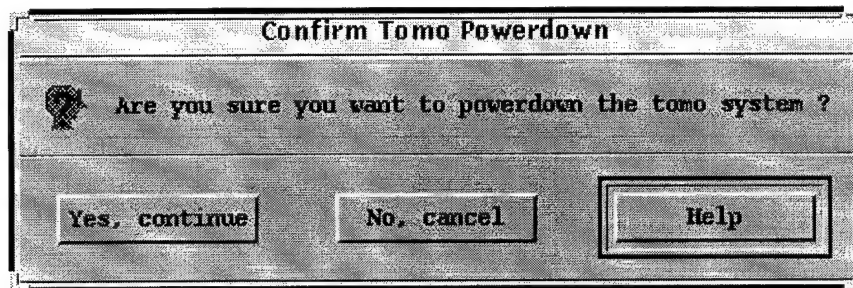


informing the operator that events are occurring.

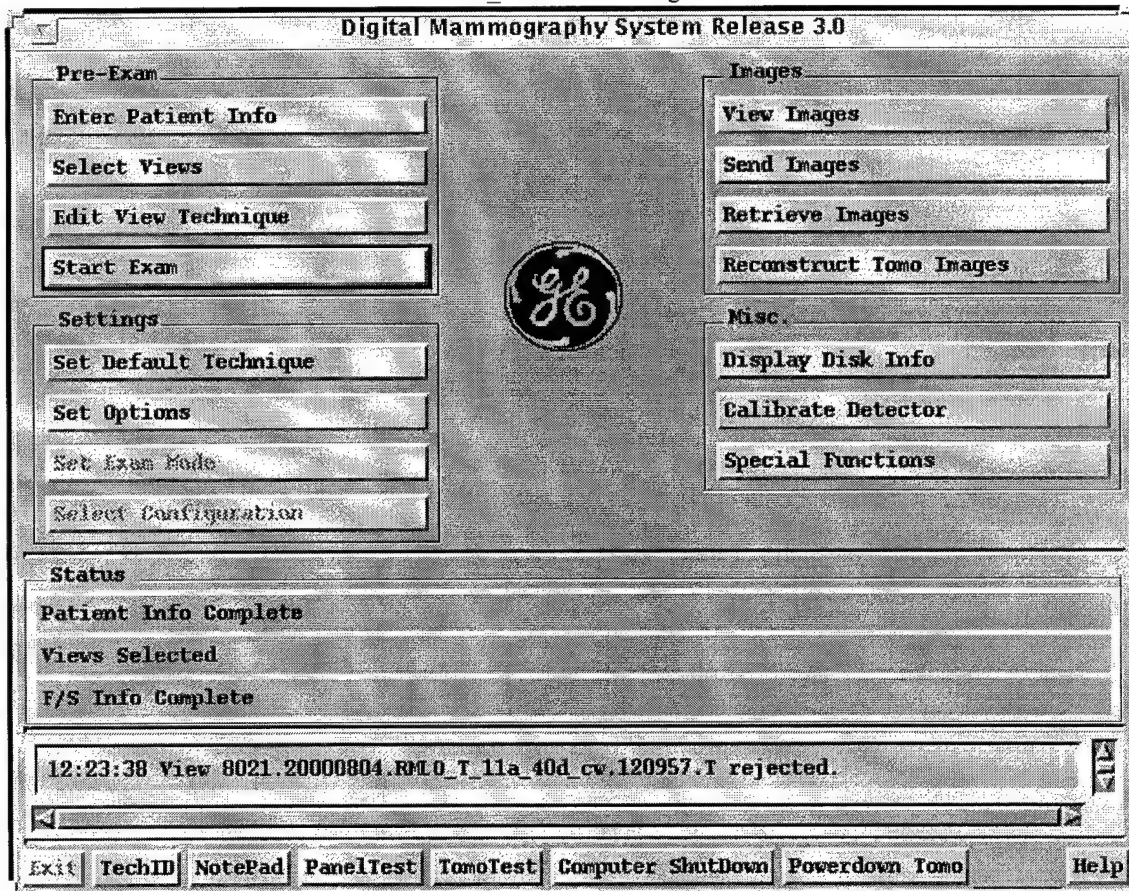


The 'Confirm Homing' widget will appear after initialization is complete. If homing is necessary and not chosen at this time, another opportunity will be presented prior to starting an exam. If homing is not allowed at that time, no exams will be possible. After the interaction with the motion control system is over, other operations are possible just as for the FFDM dms system. If dms\_tomo was previously shut down and the VME box left powered, homing may not be necessary.

The Main Widget differs from the dms version in that a button for tomo reconstruction has been added (Reconstruct Tomo Images), as well as two buttons for interacting with the motion control subsystem, and the Archive/Delete Images button has been removed (archiving is now automatically done after midnight Sunday night. The first of these new buttons on the bottom bar, is 'TomoTest' for startup operations, and the second is 'Powerdown Tomo'. The tomo drive system should not be left energized in the prolonged absence of an operator, and selecting this second button will cause the motor drives to be deenergized. **If the DMR is turned off, it is not necessary to 'Powerdown'.** If dms\_tomo is left running after a 'Powerdown', selecting 'TomoTest' and homing the drives will reset the motion control system so that exams are again possible. The 'Quality Control' button has been renamed 'Special Functions' as other functions also are available on that menu.



dms\_tomo Main Widget

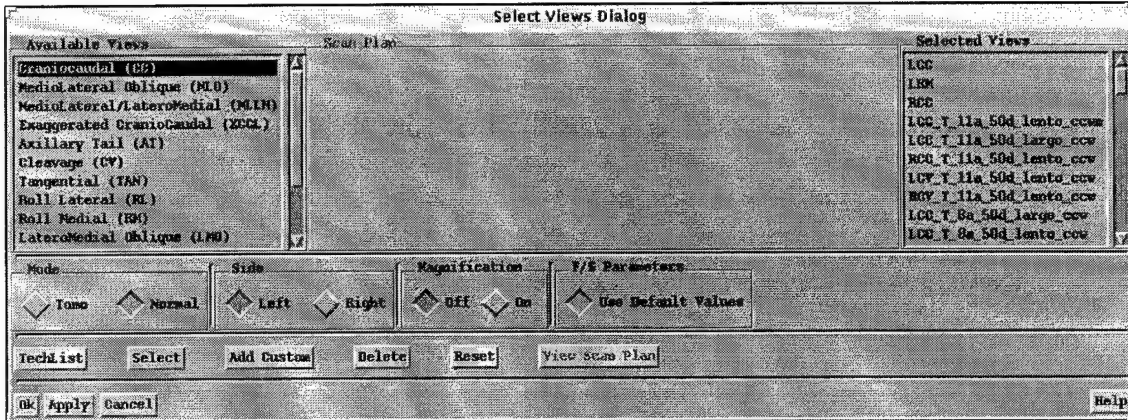


### 3-2-1 Set Default Technique

This widget affects only defaults for standard FFDM exams. The SID is fixed at 660 mm and magnification is not possible for the tomo prototype.

### 3-2-3 Select Views Widget

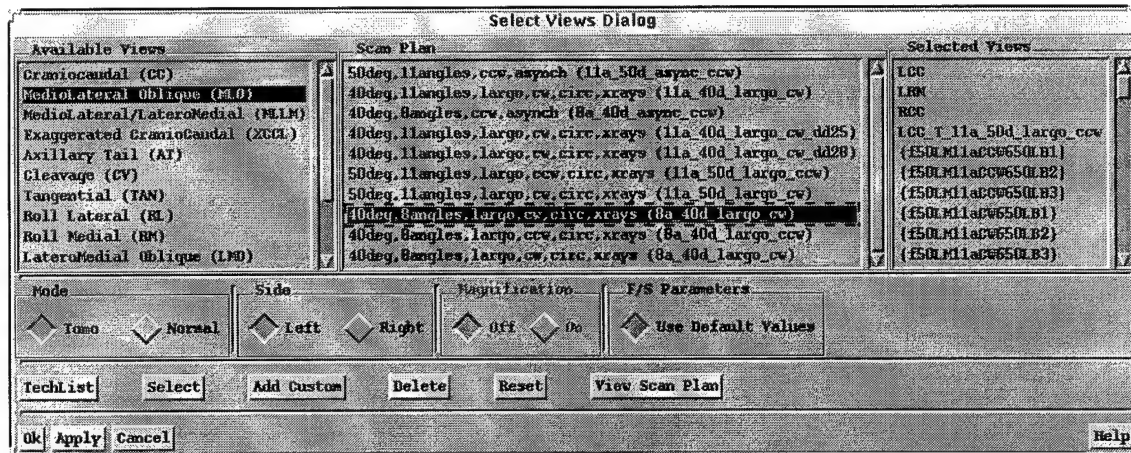
This widget allows the selection of either standard or tomo exam views. The default choice is in the standard or normal mode. The central region, for listing of tomo scan



plans, is blank.

### Normal Mode Select Views Widget

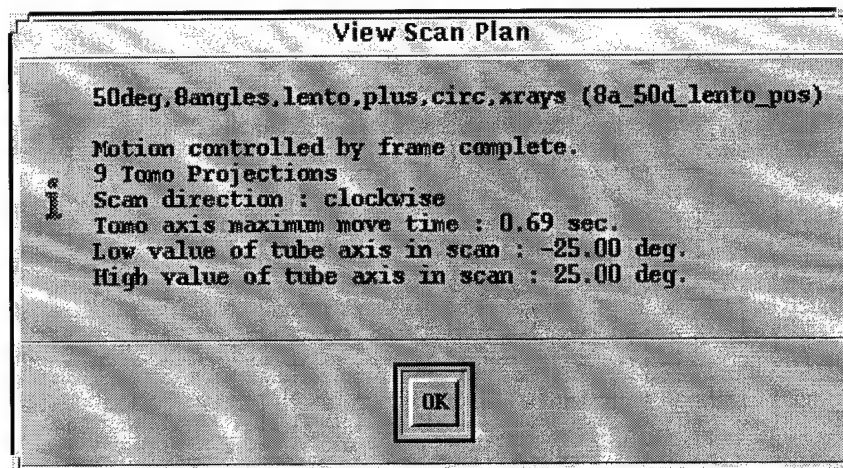
Selecting the Tomo mode results in the widget modifications shown below.



### Tomo Mode Select Views Widget

To set up a tomo view, a clinical view must be selected from the first column and a scan plan from the second, resulting in both being in reverse color, and then clicking the 'Select' button, which will generate an entry in the Selected Views column. If one desires to change the scan plan, one must delete the view from the Selected Views column and start afresh. The scan plans are characterized by the number of angles, the angular range covered, the direction of tube motion (clockwise or counter clockwise from in front of the DMR), the time for moving between the angles, and the means of causing the exposure of each frame to commence. Only choices of 8 and 11 angles are allowed; eight being the minimum useful for a tomo scan and 11 being the maximum number useful for reasonable mAs. The value of mAs for which the

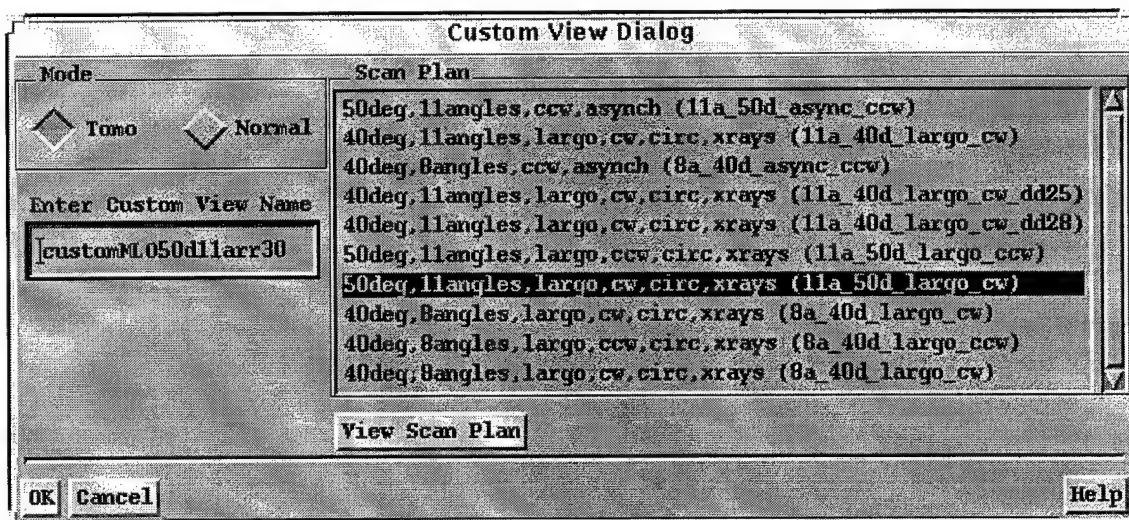
system will perform satisfactorily rises non-linearly with the number of exposures. The scans are identified as either tomo or asynch scans. For the former, the exposure of all frames after the first commences as soon as the tube motion is complete, and the graphe button must remain pressed during the entire exam until the triple beep is heard. For asynch scans, the prepa and graphe buttons must be pressed for each frame. This type of scan plan allows for system vibrations caused by tube motion to die down before the next exposure at the cost of increased exam time and risk of patient motion. The operator must wait for the motion to cease before beginning the exposure. For Tomo mode, additional information on the Scan Plan is available by clicking on the "View Scan Plan" button:



### View Scan Plan Widget

All non-asynch scan plans now have a move time of 0.64 seconds for best operation.

Custom views may be generated by clicking on the 'Add Custom' button on the Select Views Widget.



### 3-2-4 Edit View Technique Widget

The normal mode 'Edit View Technique' Widget

**View Technique Editor**

View Name: LCC - ammo

**Spot Size**

☒ Large ☐ Small

**Target**

☒ Molybdenum ☐ Rhodium

**Filter**

☒ Molybdenum ☐ Rhodium ☐ Aluminum

**kV Setting**

30

**mAs Setting**

20 List

**Magnification**

☒ OFF ☐ ON

**SID**

☒ 510 ☐ 560 ☐ 610 ☐ 660

**Grid Status**

☒ Grid ☐ No Grid

**Pixel Size**

☒ 100 ☐ 50

**Comment (optional)**

has been joined by the Tomo mode widget

**View Technique Editor**

View Name: t0d1lagridon1 - tomo

Target	Filter	kvp	mas
Mo	Mo	24	125
Mo	Mo	26	140
Mo	Mo	28	140
Rh	Rh	28	110
Rh	Rh	30	110
Rh	Rh	32	110
Mo	Rh	24	140

Comment (optional)

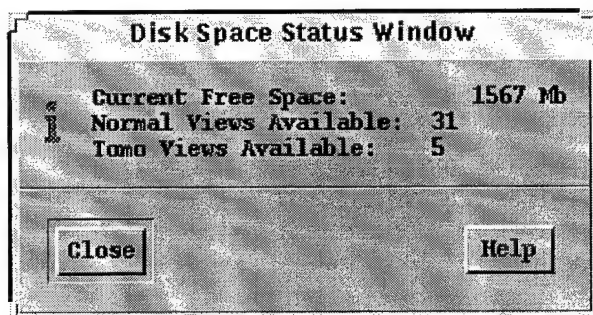
Ok Apply <<< >>> Cancel Help

which displays only those choices for which the system will operate satisfactorily. The widget shown above shows the choices available for 11 angle scans; for 8 angle scans the same target, filter, and kVp combinations are shown with the mAs values being somewhat lower. As mentioned above, it is not possible to change the scan plan for a view (the view must be deleted and re-created with the new scan plan). As before, the operator may switch from view to view for editing a sequence by clicking the 'Apply'

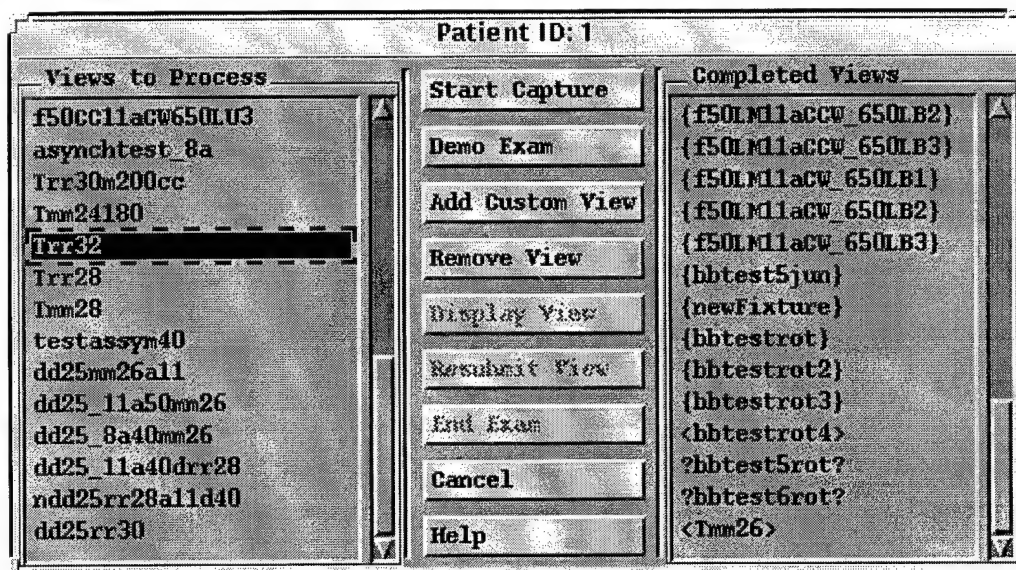
button and then either the '<<<' or '>>>' buttons to progress to the next. The proper View Technique editor will appear for the next view.

### 3-2-5 Start Exam Window

When the 'Start Exam' button is pressed on the Main Widget, a widget will appear informing the operator of the file space available for exams, usually on top of the Exam Widget. The tomo exam with 9 to 12 frames will require much more space than normal mode exams. Be sure that enough space is shown to accomplish all views plus margin for repeats before commencing an exam. The FileSpace Widget is shown below:



The Exam Widget is nearly identical to that for the FFDM prototype, except that the

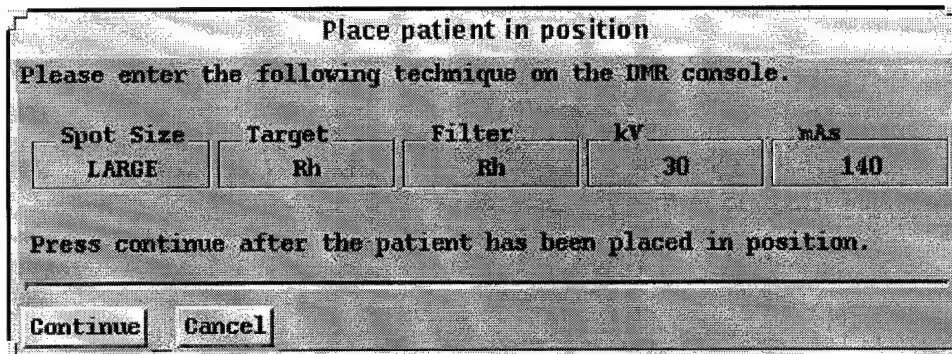


Exam Widget

button for 'Stop Capture' has been replaced by the 'Demo Exam' button'. The Stop Capture function has been moved to the Mammox widget (see below). The Demo Exam button will cause the gantry to go through a scan without x-rays, and is available for use in acquainting the patient with the sounds and sequence of the tomo exam.

However, since the motion controller must place the tube and collimator for positioning the patient, the 'Move to Zero Position' widget will appear when the 'Start Capture' button is pressed, mainly to remind the operator to warn the patient of impending motor sounds. If for some reason the tube etc. are in zero position the widget will not appear. The move to zero is required so that the light field can be used to position the patient.

Next, the Position Patient Widget will appear, instructing operator to position the patient . The DMR settings are given on it to expedite the acquisition.



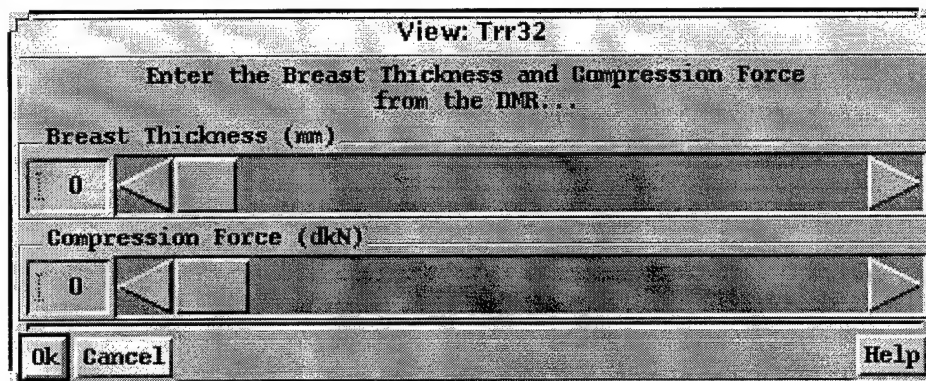
**Place patient in position**  
Please enter the following technique on the DMR console.

Spot Size	Target	Filter	kV	mAs
LARGE	Rh	Rh	30	140

Press continue after the patient has been placed in position.

**Continue** **Cancel**

When the Continue button on the Place patient widget is pressed the widget to record the breast thickness and compression force appears:



**View: Trr32**  
Enter the Breast Thickness and Compression Force from the DMR...

**Breast Thickness (mm)**

0 [Slider]

**Compression Force (dkN)**

0 [Slider]

**Ok** **Cancel** **Help**

Since the breast thickness is used to set the default reconstruction stop dimension, it should be entered accurately. Values can be entered in the text boxes on the left or by adjusting the sliders.

The actual exposure is initiated with the operation of the prepa and graphe buttons as for FFDM. The Mammox widget appears and records system progress. It automatically closes when the acquisition is complete. The information appearing in it is recorded in the ".acq.log" file, which appears first in the 'new/patient#' directory until the image is accepted or rejected, and then moved to the 'archive/patient#' directory, both under /data/dms.

The 'Demo Exam' mentioned above is provided for test purposes and is available to demonstrate the scanner operation to the patient, if desired. No x-rays are generated as the tube goes through its sequence of motions, but the noise and vibration are the same as in a view using the 50 degree range 11 angle scan plan.

### 3-2-11 Reconstruct Images Widget

The Reconstruct Images Widget allows selection of projection files for reconstruction. The projection data may be chosen from current data (not yet archived) by selecting the 'New' radio button, from archived data by selection of the 'Retrieve' button, or from previously failed reconstructions. Once a source of projections is chosen, the patient ID's available for that choice will be shown in the first column. Once a patient ID is selected, the available files will be displayed. By default all will be selected as reconstruction candidates (under the assumption that all tomo data taken is ultimately desired to be reconstructed). Files

will be placed in the third column once the reconstruction parameters are chosen by the 'Apply' button in the lower section of the form. Default parameters are listed, which include the full volume of the detector, default slice separation of 1 mm, and use of the 'shift and add' reconstruction algorithm. If only a portion of the full volume (restricted either in area or height or both), or use of a different slice separation is desired in the reconstruction, the 'Custom' radio button should be selected and the desired values entered in the appropriate place. These values will apply to all files selected at the time the 'Apply' button is pressed.

Once files appear in the 'to be reconstructed' column, they may be re-ordered via the 'Move to Top' and/or

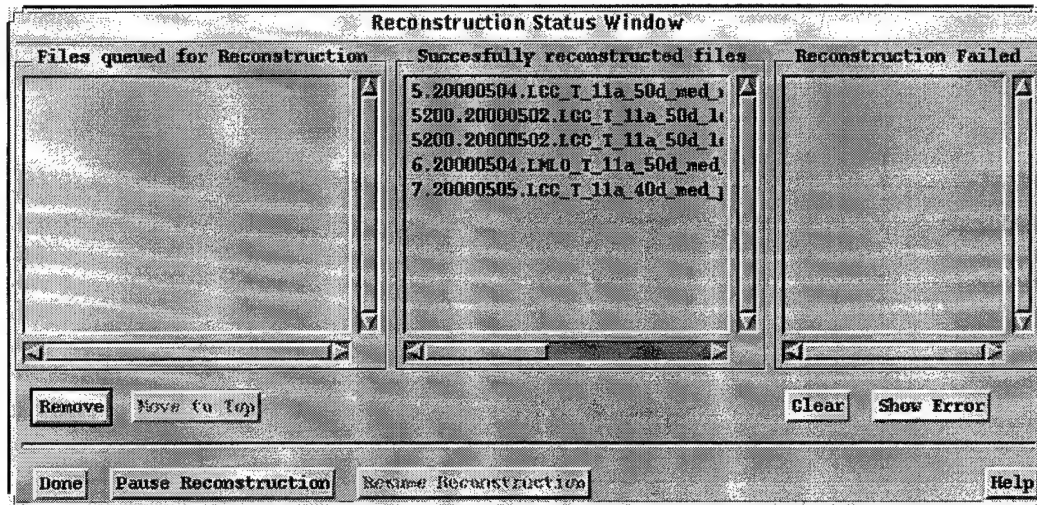
The screenshot shows the 'Reconstruction Tomo Images Window'. At the top, there are three radio buttons: 'Directory' (selected), 'New', and 'Retrieve'. Below this is a 'Reconstruction Failed' button. The main area is divided into three columns: 'Patient ID', 'Available files for reconstruction', and 'Files to be reconstructed'. The 'Available files' column lists 10 files with their corresponding Patient IDs (1, 2, 3, 5, 6, 7, 666, 667, 5200, 50898). Below the columns are 'View Image', 'Remove', and 'Move to Top' buttons. The 'Parameters' section at the bottom has two radio buttons: 'Default' (selected) and 'Custom'. It contains input fields for 'Start Row (pixels)' [0], 'Start Column (pixels)' [0], 'Stop Row (pixels)' [2303], 'Stop Column (pixels)' [1799], 'Start Height (cm)' [1.00], 'Stop Height (cm)' [2.00], and 'Slice Separation (cm)' [0.10]. There are also three radio buttons for 'Algorithm Type': 'algo1' (selected), 'algo2', and 'algo3'. At the bottom of the window are buttons for 'Start Later', 'Start Now', 'Status', 'Set Recon Later Time', 'Cancel', and 'Help'.

'Remove' buttons, which will affect the reverse-video 'selected' data sets.

The time at which reconstructions begin is selectable via the buttons at the bottom of the form, with the time for 'Start Later' set by clicking on the 'Set Recon Later Time' button which brings up the simple 'Set Recon Later Time' widget.

The screenshot shows the 'Set Reconstruction Start Later Time' dialog box. It has a title bar with the same text. Inside, it says 'Time to start reconstruction 12:00 AM'. Below this is a 'Change Time' section with three radio buttons: 'Hour' (selected), 'Minute', and 'AM/PM'. There are also two arrow buttons (up and down) for adjusting the time. At the bottom are 'OK', 'Cancel', and 'Help' buttons.

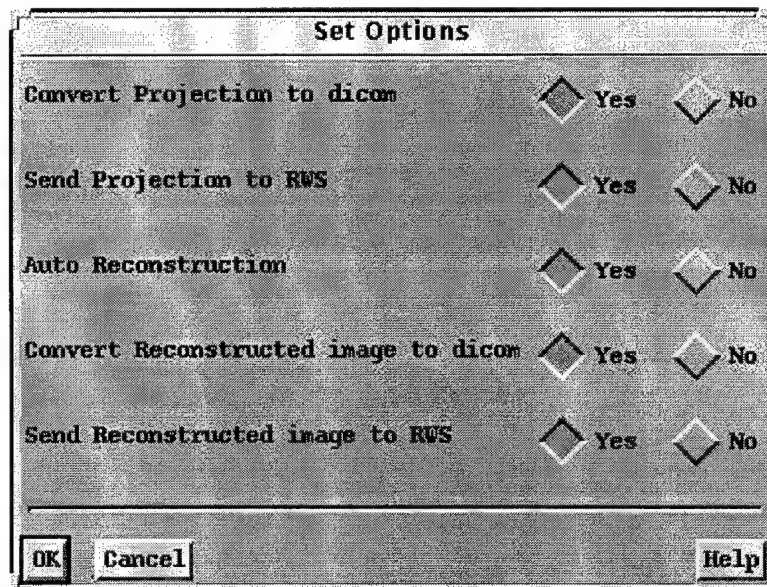
The status of datasets submitted for reconstruction can be observed and modified by using the widget brought up by the 'Status' button:



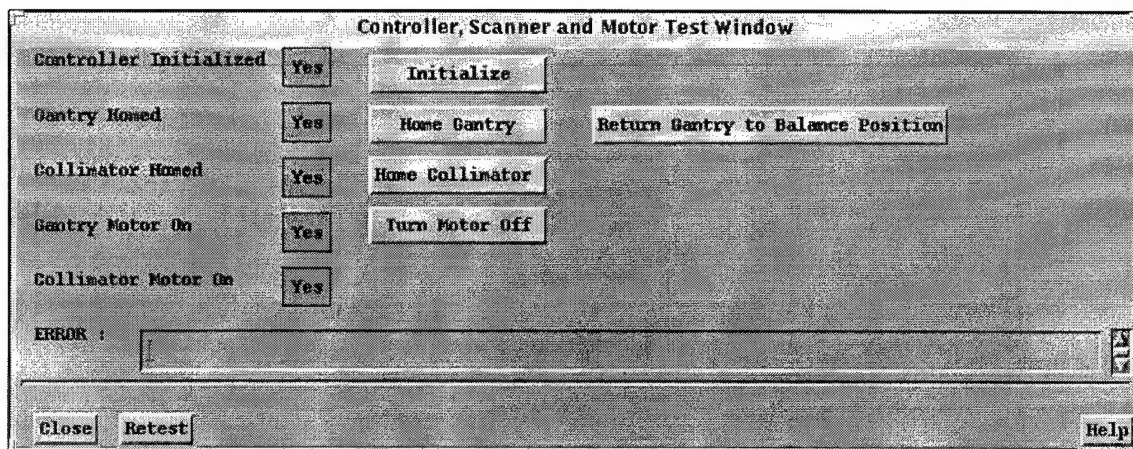
Files queued can be removed from the queue or re-prioritized; the reconstruction process can be paused if it is affecting other processes such as acquisition or image viewing.

### 3-2-12 Set Options Widget

This widget sets the options for creating dicom files and sending them to the review workstation and for enabling/disabling automatic reconstruction of tomo data sets. If settings other than the default (all 'Yes') are desired, they should be set before any images are created. If the settings are changed during a session, the changes will apply to all images created after the changes are made.



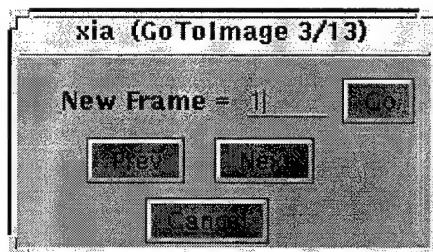
### 3-2-13 Motion Controller Interaction Widget



All indicators must be a green 'YES' for the system to function properly. Pressing 'Initialize' should turn motors on if necessary (the DMR must be on for motion to occur), and pressing a 'Home' button will home the selected axis. If the gantry is left at then end of some operation in other than the 'Balance Position', such that the green light emitting diodes near the gantry rotation switch are not lit, pressing the 'Return Gantry to Balance Position' button should complete the operation.

#### **Section 4 Image Examination using xia**

xia has been enhanced for multiple image data sets, either projections or reconstruction. The primary change is that xia has the ability to randomly access frames in a multiple frame dataset, using the 'frame' widget invoked by typing 'f' in the xia window. As illustrated below, the current frame number and number of frames in the data set are indicated at the top of the widget.



xia Frame Widget

Additionally, if the image has been panned, and another frame is selected for viewing, the pan is preserved so that structures can easily be tracked from one frame to the next.

#### **Maintenance**

##### **Section 1 Performance Checks**

Monthly a check of the gantry brake should be performed by turning on the inclinometer with the gantry positioned for a CC exam. Load an arbitrary patient and 'Start Exam'. Read and record the inclinometer angle, and using the Demo Exam feature, run the gantry 10 times. Read and record the inclinometer angle again, and if it differs from the initial reading by more than 0.1 degrees, call CRD.

## **Section 2 Other Maintenance Operations**

Only maintenance discussed for the FFDM should be done. Call CRD if any problems occur with the motion control system.

## **Section 3 CRD contact list**

Michael Denvir (518) 387-4113

Jeff Eberhard (518) 387-4301

## **Appendix 4: Patent Application by GECRD**

# REPORT OF INVENTIONS AND SUBCONTRACTS

Form Approved  
OMB No. 5000-0095  
Expires July 31, 1985

Public reporting burden for this collection of information is estimated to average 1 hour per response, including the time for reviewing instructions, searching existing data sources, gathering and maintaining the data needed, and completing and reviewing the collection of information. Send comments regarding this burden estimate or any other aspect of this collection of information, including suggestions for reducing the burden, to Washington Headquarters Services, Directorate for Information Operations and Reports, 1215 Jefferson Davis Highway, Suite 1204, Arlington, VA 22202-4302, and to the Office of Management and Budget, Paperwork Reduction Project (5000-0095), Washington, DC 20503.

(Pursuant to "Patent Rights" Contract Clause) (See Instructions on Reverse Side.)

PLEASE DO NOT RETURN YOUR COMPLETED FORM TO EITHER OF THESE ADDRESSES. RETURN COMPLETED FORM TO THE CONTRACTING OFFICER.

1a. NAME OF CONTRACTOR / SUBCONTRACTOR GENERAL ELECTRIC COMPANY	c. CONTRACT NUMBER DAMD179818309	2a. NAME OF GOVERNMENT PRIME CONTRACTOR Massachusetts General Hospital	c. CONTRACT NUMBER 120078200571	3. TYPE OF REPORT (X one) a. INTERIM <input checked="" type="checkbox"/> b. FINAL <input type="checkbox"/>
b. ADDRESS (include ZIP Code) Corporate Research & Dev.	d. AWARD DATE (YYMMDD) 990104	b. ADDRESS (include ZIP Code) 55 Fruit Street Boston, MA 02114	d. AWARD DATE (YYMMDD) 990104	4. REPORTING PERIOD (YYMMDD) a. FROM: 990104 b. TO: 032900

## SECTION I - SUBJECT INVENTIONS

NAME(S) OF INVENTOR(S) (Last, First, M.I.)	TITLE OF INVENTION(S)	DISCLOSURE NUMBER, PATENT APPLICATION SERIAL NUMBER OR PATENT NUMBER	PATENT APPLICATIONS				CONFIRMATORY INSTRUMENT OR ASSIGNMENT FORWARDED TO CONTRACTING OFFICER
			(1) UNITED STATES		(2) FOREIGN		
Wang, Yu Wirth, Reinhold Alexander, James P.	TOMOSYNTHESIS X-RAY MAMMOGRAM DRIVE SYSTEM AND SUPPORT STRUCTURE -X-RAY TUBE ON AN ARC TRACK	RD-27970	(a) YES <input checked="" type="checkbox"/>	(b) NO <input type="checkbox"/>	(a) YES <input type="checkbox"/>	(b) NO <input type="checkbox"/>	(1) YES <input type="checkbox"/> (2) NO <input type="checkbox"/>

## 1. EMPLOYER OF INVENTOR(S) NOT EMPLOYED BY CONTRACTOR / SUBCONTRACTOR

(1) (a) NAME OF INVENTOR (Last, First, M.I.)

(1) TITLE OF INVENTION

2. ELECTED FOREIGN COUNTRIES IN WHICH A PATENT APPLICATION WILL BE FILED

(2) FOREIGN COUNTRIES OF PATENT APPLICATION

(b) NAME OF EMPLOYER

(b) NAME OF EMPLOYER

(c) ADDRESS OF EMPLOYER (include ZIP Code)

(c) ADDRESS OF EMPLOYER (include ZIP Code)

## SECTION II - SUBCONTRACTS (Containing a "Patent Rights" clause)

a. SUBCONTRACTS AWARDED BY CONTRACTOR/SUBCONTRACTOR, (If "None", so state)

NAME OF SUBCONTRACTOR(S)	ADDRESS (include ZIP Code)	SUBCONTRACT NUMBER(S)	DFAR "PATENT RIGHTS"		DESCRIPTION OF WORK TO BE PERFORMED UNDER SUBCONTRACT(S)	SUBCONTRACT DATES (YYMMDD)	
			(1) CLAUSE NUMBER	(2) DATE (YYMM)		(1) AWARD	(2) ESTIMATED COMPLETION
NONE							

## SECTION III - CERTIFICATION

7. CERTIFICATION OF REPORT BY CONTRACTOR / SUBCONTRACTOR. (Not required if

Small Business or

Non-Profit organization.) (X appropriate box)

a. NAME OF AUTHORIZED CONTRACTOR / SUBCONTRACTOR OFFICIAL (Last, First, M.I.)  
Snyder, Marvin

c. I certify that the reporting party has procedures for prompt identification and timely disclosure of "Subject Inventions," that such procedures have been followed and that all "Subject Inventions" have been reported.

b. TITLE Patent Counsel - Electronics and Mechanical

d. SIGNATURE

*Marvin Snyder*

\* DATE SIGNED

3/30/84

1718  
**DISCLOSURE LETTER OUTLINE**

20  
**Distribution:**

Patent Operation  
Original & 2 Copies\*  
via Lab Manager  
Immediate Manager  
Inventors: Y. Wang  
R. Wirth, J. Alexander

Building \_\_\_\_\_ Room: \_\_\_\_\_  
Date: \_\_\_\_\_

Laboratory Manager of each inventor: \* Jan Aase  
Bruce Griffing

**SUBJECT: PATENT DISCLOSURE LETTER**

on: Tomosynthesis X-ray Mammogram Drive System and Support  
Structure - X-ray Tube on an Arc Track

1. **OBJECT OF INVENTION** (e.g., problem, opportunity, prior art)

X-ray mammograms technology utilize a rotational X-ray supporting frame which can position the X-ray tube in any angle between the vertical to horizontal position to perform the scans. The tomosynthesis technology requires the X-ray tube be automatically moved and positioned in a sequence of angle increments in one scan. One of the biggest challenges in a tomosynthesis structure is the induced vibration from the step motion of X-ray tube. To reduce the total scan time, the X-ray tube motion must be fast (0.1-0.5sec/step). The high speed step-motion then introduce significant impulsive forces during the scan and induces structural vibration. The vibration will reduce the image quality. The system vibration is the primary limitation to the drive options. The precision of the move is also a key requirement. The following concept produces low dynamic forces during the scan, thus induces low system vibration.

2. **DESCRIPTION OF INVENTION**

The magnitude of dynamic forces resulted from system step motion is linearly proportional to the motion acceleration and the mass in motion. The proposed supporting structure will minimize the mass in motion by introducing an arc track with only X-ray tube move during the scan. The concept also reduces the driving power, thus the size and the weight of the motor. The entire supporting structure can be rotated manually into either horizontal or vertical position. The X-ray tube position is controlled by the precise arc shape track. A step motion driving source can be produced either from a shaft torque through a driving arm or from an attached motor on the track. The arc center could be either at the shaft center or at the detector location for the optimization of the field of view.

3. **OTHER INFORMATION** (e.g., test data, reduction to practice, planned use)

Conceptual design was conducted in August 1999.

4. **RECORDS**

The idea was discussed in several of the team meetings and refined by analysis. The concept was recorded on page 11 of Yu Wang's bound note book on 7 May 99.

\* Disclosure Letter should be addressed to Lab Manager of each inventor.

Page: 1 Date:

M. J. Angler  
2/17/00

AD-27970

5. WITNESSES AND DATE

READ AND UNDERSTOOD BY:

WITNESS: *Michael S. Gh*  
Signature

Date: 2/15/00

READ AND UNDERSTOOD BY:

WITNESS: *John A. Abal*  
Signature

Date: 2/21/00

READ AND UNDERSTOOD BY:

WITNESS: *EW Balch*  
Signature

Date: 3/7/00

READ AND UNDERSTOOD BY:

WITNESS:  
Signature

Date:

READ AND UNDERSTOOD BY:

WITNESS:  
Signature

Date:

\*INVENTOR: *Yu Wang*  
Signature

Yu Wang

CRD Engineering Mechanics Lab  
Laboratory or Program

Date: 2/14/2000

\*INVENTOR: *Reinhold F Wirth*  
Signature

Reinhold Wirth

CRD Industrial Electronics Lab  
Laboratory or Program

Date: 3/2/00

\*INVENTOR: *James Alexander*  
Signature

James Alexander

CRD Engineering Mechanics Lab  
Laboratory or Program

Date: 2/14/00

\*INVENTOR:  
Signature

Laboratory or Program  
Date:

\*INVENTOR:  
Signature

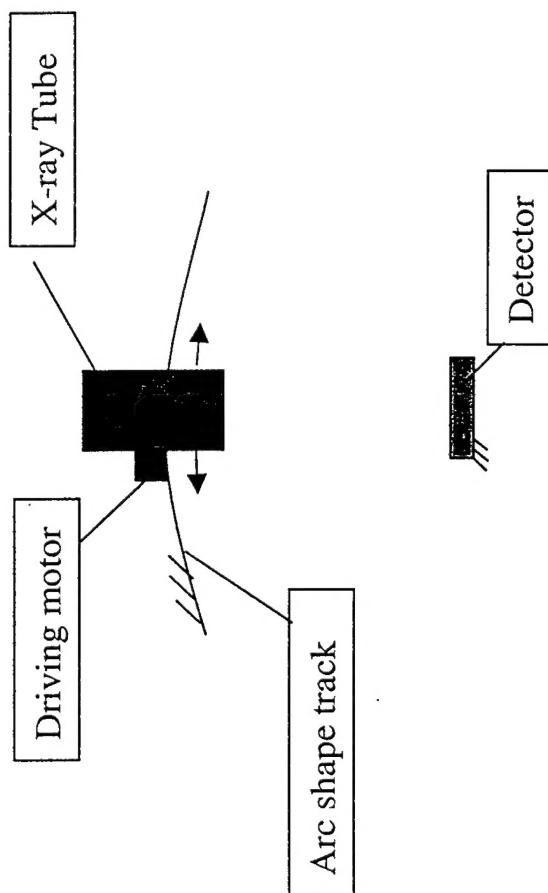
CRD Industrial Electronics Lab  
Laboratory or Program  
Date:

\*When the invention is joint, all inventors should sign and date the disclosure letter.  
(Complete and attach an Invention Disclosure Statement, Form RD-506A, for each inventor.)

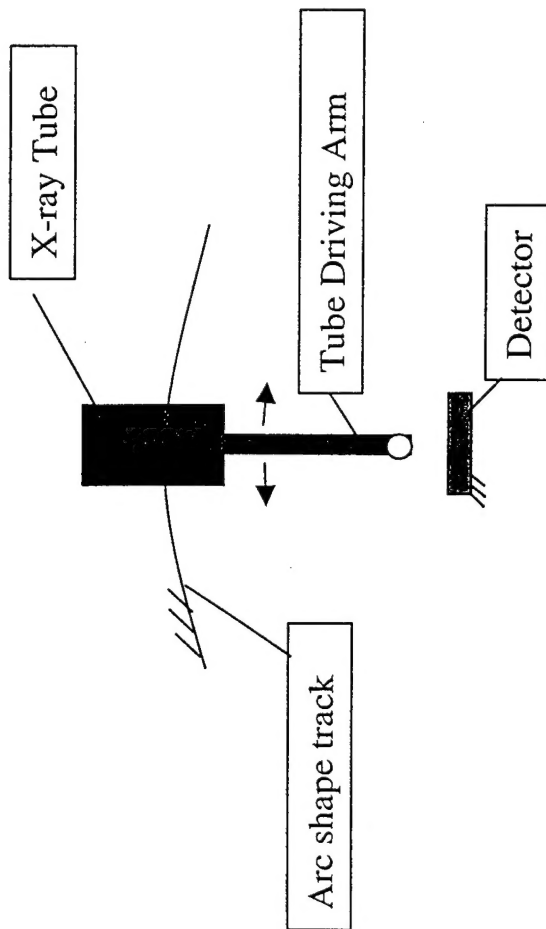
Print hard copy for signatures and deliver to Patent Operation.

MS  
3/17/00

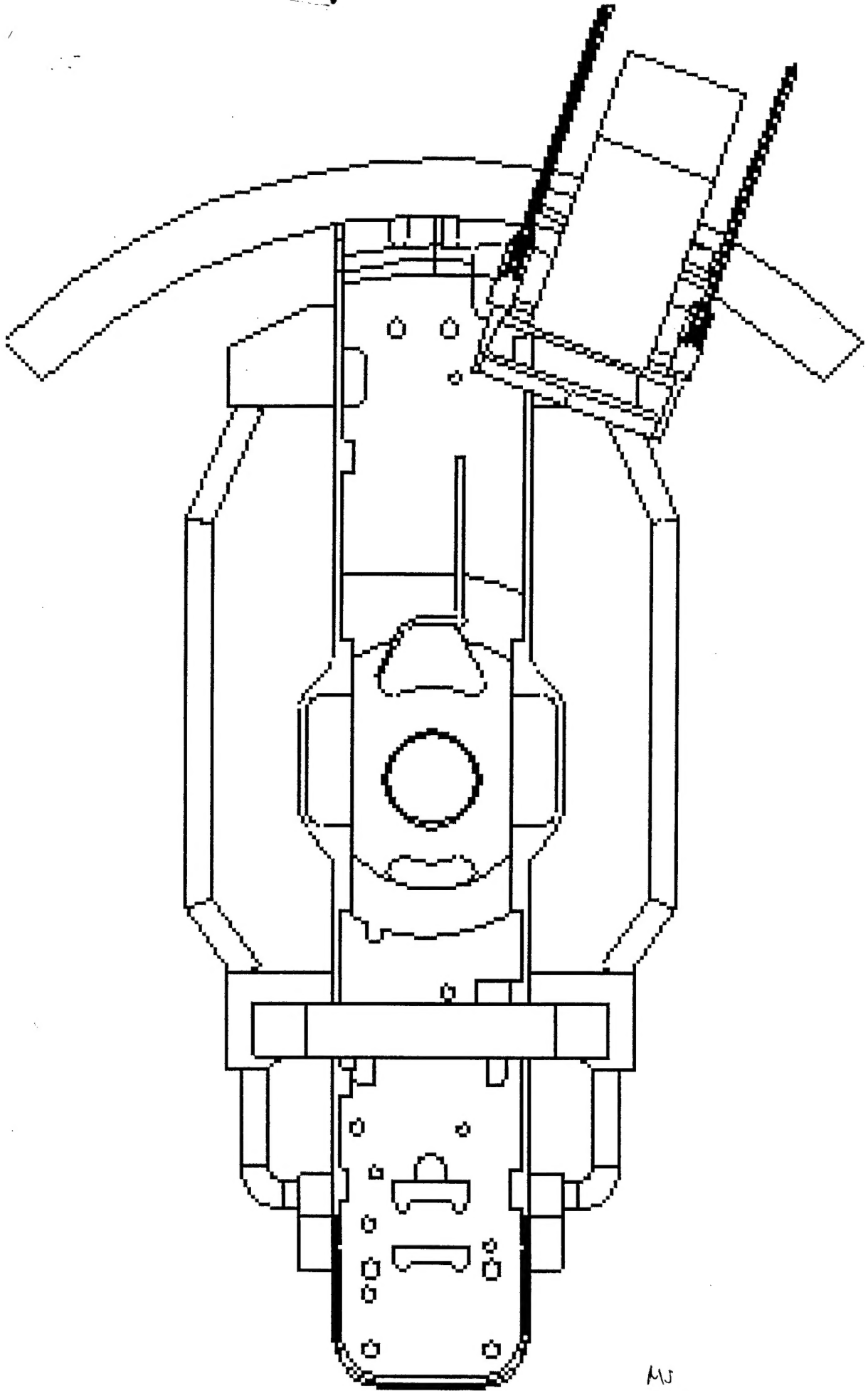
RD-27970



MS  
3/17/20



AW  
3/17/82



MS  
3/17/00  
RD-27970